Adaptive Power Control for Energy Harvesting Communication Systems

by

Masoud Badiei Khuzani

A thesis
presented to the University of Waterloo
in fulfillment of the
thesis requirement for the degree of
Master of Applied Science
in
Electrical and Computer Engineering

Waterloo, Ontario, Canada, 2013

I hereby declare that I am the sole author of this thesis. This is a true copy of the thesis, including any required final revisions, as accepted by my examiners.

I understand that my thesis may be made electronically available to the public.

Abstract

Sustaining energy requirement for wireless devices is the main barrier in building autonomous communication systems and service-free networks. Specifically, in large-scale networks where normally wired energy infrastructures are unavailable, regular battery maintenance for each individual node is inefficient or unfeasible.

To resolve this problem, current and future state of the art technologies are focused on development of perpetual energy resources by harvesting free energy in the environment such as kinetic, thermal, solar, or wind energies. However, the integration of energy harvesting architectures with communication systems requires innovating adaptive transmission power policies.

In this thesis, we investigate the structure of efficient transmission power policies for a multiple access communication system with energy harvesting nodes where the utility function is taken to be the long-term average sum-throughput. We assume a causal structure for energy arrivals and study the problem in the continuous time regime. For this setting, we first characterize a *storage dam* model that captures the dynamics of a battery with energy harvesting and variable transmission power. Using this model, we next establish an upper bound on the throughput problem as a function of battery capacity.

We also formulate a non-linear optimization problem to determine optimal achievable power policies for transmitters. Applying the calculus of variation technique, we derive Euler-Lagrange equations as necessary conditions for optimum power policies in terms of a system of coupled partial integro-differential equations (PIDEs). Based on a Gauss-Seidel algorithm, we then devise an iterative algorithm to solve these equations.

Finally, we propose a fixed-point algorithm for the symmetric multiple access setting in which the statistical descriptions of energy harvesters are identical. To support our iterative algorithms, comprehensive numerical results are also obtained.

Acknowledgements

It is a pleasure to thank the many people who made this thesis possible.

Foremost, I owe my deepest gratitude to my supervisor, Professor Patrick Mitran. He has a great personality beside an amazing intellectual acuity. Certainly, he is one of the smartest people that I know. It was truly my honor to have his company in this journey. He is a great mentor, a fine scholar, and my best friend. I hope that one day I could be like him.

I am indebted to Professor Ravi Mazumdar for always finding time to discuss my questions. I was benefited from his wisdom a lot in the past two years. It was my honor to learn stochastic processes and queuing systems from him.

I would like to thank the other member of my seminar committee, Professor Amir Khandani, for his time and thoughtful comments.

I also like to thank my friends Hamidreza, Ehsan, and Meysam. They were a source of support which I could rest upon in the hard times.

Last but not least, I thank my dear family for their magnificent supports. There is no way that I can express my gratitude to them.

Dedication

To My Parents

Table of Contents

List of Tables viii

List of Figures ix

1 Introduction 1

1.1 Background 1

1.2 Energy Harvesting (EH) Systems 2

1.2.1 Overview of EH Techniques 2

1.2.2 Efficiency 5

1.3 Power Adaptation to EH Resources 7

1.4 Related Works 8

1.4.1 Energy Management 8

1.4.2 Energy Harvesting 9

1.5 Contributions 10

1.6 Thesis Organization 10

2 Online Power Policies for EH Communication over Multiple-Access Channel 11

2.1 Preliminaries 11

2.1.1 Communication model 11

2.1.2 Energy harvesting and storage model 12

2.1.3 Notation . . . 13
2.2 Ergodic Theory of Storage Process . . . 14

3 Bounds on Total Average Throughput and Achievable Schemes **18**
3.1 Introduction . . . 18
3.2 An Upper Bound . . . 19
3.2.1 Finite Storage Battery . . . 19
3.2.2 Infinite Storage Battery . . . 21
3.3 Achievable allocation scheme . . . 22
3.3.1 Infinite Storage Battery . . . 29
3.3.2 Finite Storage Battery . . . 30
3.4 Discussion and Numerical Solution . . . 35

4 Summary and Future Research **40**
4.1 Summary . . . 40
4.2 Future Research and Extensions . . . 41

APPENDICES **42**

A Optimality of Markov Power Policies **43**

B Concavity of the Objective Function Over Each Coordinate **48**

C A Lemma **51**

D Formulation of Power Policies on a Finite-Time Horizon **53**

References **57**

List of Tables

1.1 Power consumption of commercial sensor nodes [19]. 2

1.2 Power performance of energy harvesting methods [21]. 7

3.1 Total average throughput for two identical nodes, using Shannon rate function, $r(x) = \frac{1}{2}\log(1 + x/N_0)$, with $N_0 = 1$, equation constant $K = 0$, initializing function $p^{(0)}(x) = x + p(0^+), 0 < x \leq L$, and for various storage capacity L and initial values $p(0^+)$. 36

3.2 Total average throughput for two identical nodes, using Shannon rate function, $r(x) = \frac{1}{2}\log(1 + x/N_0)$, with $N_0 = 1$, initial value $p(0^+) = 0.001$, initializing function $p^{(0)}(x) = x + p(0^+), 0 < x \leq L$, and for various storage capacity L and equation constant K. The upper bound for an infinite storage battery ($L_k = \infty$) is given by $R_\infty = \frac{1}{2}\log(1 + 2) = 0.792$. 37

List of Figures

1.1 Solar spectrum (250 nm-2500 nm). The $\psi = hf$ has the corresponding range of values between 4.959 eV to 0.496 eV. (image courtesy of Wikipedia [1]). 3

1.2 Schematic of a simple radio energy harvesting module for sensor devices. . 5

1.3 The evolution of efficiency of solar cells since 1976 (credit: US department of energy [4]). 6

2.1 The balance between positive jumps from subspace $[0, x]$ and the drift component of the process. 16

3.1 Battery capacity $L = 3$, equation constant $K = 0$, and $p(0^+) = 0.1$ for two nodes case. (a) The convergence of transmission power policy to an achievable policy (denoted by squares) after $N = 10$ iterations with initializing function $p^{(0)}(x) = x + p(0^+)$ (dashed lines) and iterates (solid lines), (b) Absolutely continuous part $f(x)$ of $\pi(x)$ for the converged solution. 38

3.2 Transmission power policies $p(x)$ with different initial values ($L = 3, M = 2, K = 0$). 39

3.3 Robustness to the initializing function, using a constant initializing function (dashed line) $p^{(0)}(x_k) = p(0^+), 0 \leq x_k \leq L$ ($L = 3, M = 2, K = 0$ and $N = 10$). 39

Chapter 1

Introduction

1.1 Background

[1] The fast growing utilization of sensor devices in measurement and automation has created a new challenge, i.e., the problem of sensor maintenance. The sensor maintenance is crucial to prevent faulty measurements, and can be extremely difficult and expensive depending on the scale of sensor networks. Furthermore, a significant fraction of sensor maintenance issues are due to the battery exhaustion. Therefore, an improvement in either sensor energy consumption or battery performance returns a huge cost saving for industrial consumers.

To reduce the sensor energy consumption, various energy management strategies are proposed in the literature (for a brief survey see [5] and [39]). The main goal of those strategies is to decrease the radio activity, the number of data acquisitions, and to coordinate the sleep/wake-up times of sensor device. Table 1.1 shows the current output of the battery for different sensor tasks including data transmission, data reception, and processing.

While energy management strategies are helpful, they have limited payoff since they merely prolong the lifespan of the sensor. Furthermore, technological advancements in battery performance has been slow in comparison to advancements in silicon industries. For instance, in the period between 1990 and 2005, battery energy density has only increased by three-fold while disk storage density has increased over 1200 times [27]. Due to those problems, current state of the art technologies are focused on developing perpetual energy resources by harvesting free energy in the environment.

[1] The results of this thesis is published in IEEE Transactions on Information Theory.

Table 1.1: Power consumption of commercial sensor nodes [19].

	Crossbow MICAz	**Intel IMote2**	**Jennic JN5139**
Radio Standard	IEEE802.15.4/ZigBee	IEEE802.15.4	IEEE802.15.4/ZigBee
Typical Range	100 m (outdoor), 30 m (indoor)	30 m	1 km
Data Rate (kbps)	250 kbps	250 kbps	250 kbps
Sleep Mode (deep sleep)	15 μA	390 μA	2.8 μA (1.6 μA)
Processor Only	8 mA active mode	31-53 mA*	2.7+0.325 mA/MHz
RX	19.7 mA	44 mA	34 mA
TX	17.4 mA (+0dbm)	44 mA	34 mA (+3 dBm)
Supply Voltage (minimum)	2.7 V	3.2 V	2.7 V
Average	2.8 mW	12 mW	3 mW

*Consumption depends on clock speed selected between 13-104MHz.

1.2 Energy Harvesting (EH) Systems

1.2.1 Overview of EH Techniques

Energy harvesting is a process in which ambient energy is converted to an electrical signal. The main renewable energy sources that are currently utilized for energy harvesting in sensor devices are listed below:

- *Solar*: Solar energy can be converted to electricity by means of photo-voltaic effect. Photo-voltaic effect was first discovered by French physicist Edmund Bequerel in 1839, and was explained later by Albert Einstein in 1905. In a photo-voltaic process, electrons bounded to an atom's nucleus are ejected from the atom by the absorption of energetic photons. Those electrons are in turn able to produce current in an electric circuit. The maximum kinetic energy $K_{\max}$ of ejected electrons are calculated by Einstein relation

$$K_{\max} = h(f - f_0), \tag{1.1}$$

where $h = 4.13 \times 10^{-15}$(eV.s) is Plank's constant, f is the frequency (Hz) of emitted light, and f_0 is the minimum frequency required to excite the electrons. The function $\psi = hf_0$ is called the *work function* and is experimentally determined for different materials.

For a solar cell, the high work function of the cell material means that most of the daylight photons can not be absorbed and thus get wasted. In contrast, when the work function is too small, the generated voltage across the circuit becomes small as ejected electrons have a small kinetic energy. The optimal value for the work function is computed to be 1.4 eV ($\sim$ 850 nm) with respect to the sunlight (see Fig. 1.1) [25]. For a crystalline silicon, the work function is 1.1 eV ($\sim$ 1100 nm) which is close to the optimal value. As a result, most of solar cells are built from silicon materials.

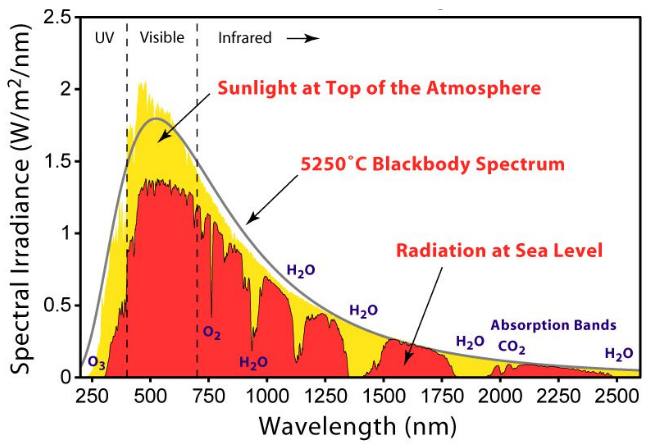

Figure 1.1: Solar spectrum (250 nm-2500 nm). The $\psi = hf$ has the corresponding range of values between 4.959 eV to 0.496 eV. (image courtesy of Wikipedia [1]).

It is worthwhile to mention that the first photo-voltaic module was built by Bell laboratories in 1954 and was exploited by NASA for space programs in 1960s [2].

- *Thermal*: In this approach, the temperature gradient results in the diffusion of electrons from a hot metal junction to a cold one. This phenomena is called the Seebeck effect in honor of German physicist Thomas Johann Seebeck who first discovered it in 1821 while investigating the thermal effect on galvanic arrangements. In particular, the voltage gradient ∇V is related to the temperature gradient ∇T as follows

$$\nabla V = S \nabla T, \tag{1.2}$$

where S (V/K) is the Seebeck coefficient.

- *Vibration*: The underlying physical phenomenon behind this method is the piezoelectric effect. Piezoelectricity was discovered in 1880 by Pierre Curie and Jacques Curie. In this process, an external stress deforms each molecule in the structure of a piezoelectric material, creating a dipole. The accumulation of these dipoles produces a net charge on the polarization surface of the piezoelectric material. Moreover, the piezoelectricity is reversible in the sense that if an electric field is applied to a piezoelectric material, it results in mechanical stress. The piezoelectric effect occurs in mono-crystalline materials as well as in poly-crystalline ferroelectric ceramics. The mathematical modeling of the piezoelectric effect can be provided by combining

- The materials electrical behavior: $D = \epsilon E$
- Hook's law: $S = sT$

where

D: electric displacement ($\mathrm{C/m^2}$)

E: electric field strength (N/C)

ϵ: permittivity ($\mathrm{C^2/N.m^2}$)

S: strain (1/m)

T: stress ($\mathrm{N/m^2}$)

s: compliance (m/N)

In particular, we have the following tensor equations

$$\begin{aligned} D &= [\epsilon^T]E + [d]T \qquad \text{(Direct piezoelectric effect)} \\ S &= [s^E]T + [d^t]E, \quad \text{(Reverse piezoelectric effect)} \end{aligned}$$

where $[d]$ is the matrix of piezoelectric effect with $d_{ij,k} = \partial S_{ij}/\partial E_k$, and $[d^t]$ is the matrix of reverse piezoelectric effect.

- *Radiation*: The idea of harvesting energy from ambient radio waves originates from Heinrich Hertz who successfully demonstrated the presence of electromagnetic waves by building an apparatus that produced and detected VHF/UHF radio waves. A simple arrangement for harvesting ambient radiation is shown in Fig. 1.2.

  The accessible power density $\mathscr{P}_D(\mathrm{W/m^2})$ to a radio energy harvesting module at a distance R from the transmitter is given by [45]

$$\mathscr{P}_D = G_T P_T / 4\pi R^2, \tag{1.3}$$

  where P_T (W) is the average transmission power, and G_T is the antenna gain of the transmitter. In particular, G_T determines the figure-of-merit of an antenna to convert the input power to radio waves [45], i.e.,

$$G_T := \frac{\text{Maximum radiation intensity of actual antenna}}{\text{Radiation intensity of isotropic antenna with the same power input}}. \tag{1.4}$$

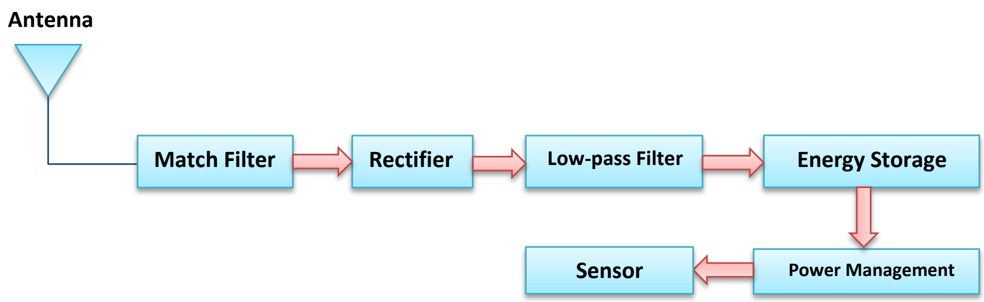

Figure 1.2: Schematic of a simple radio energy harvesting module for sensor devices.

1.2.2 Efficiency

The energy conversion efficiency η (dimensionless) of an energy harvesting process is defined as the ratio of the power output of the transducer P_{out} to the power input P_{in}, i.e.,

$$\eta = \frac{P_{\text{out}}}{P_{\text{in}}}. \tag{1.5}$$

The efficiency η of a transducer largely depends on the nature of exogenous energy resource. In the case of solar panels, the η efficiency under standard test conditions (temperature: 25°, irradiance: 1000 W/m^2, air mass: 1.5d) has a range between 6% for amorphous silicon-based solar cells up to 44.7% with multiple dies assembled into a hybrid package[2]. Fig. 1.3 shows the evolution of the solar cell efficiency since 1976. A thermodynamic limit of Photovoltaic energy conversion is derived in [12]. Specifically, a hypothetical solar panel with an infinite stack of p-n junctions and with smoothly varying bandgap is studied. It was shown that the maximum efficiency of this structure (which yields an upper bound on η) under constant emission-temperature operation is described by

$$\eta_{\text{max}} = \left(1 - \frac{T_c}{T_0}\right)\left[1 - \left(\frac{T_0}{T_s}\right)^4\right], \tag{1.6}$$

where T_c is the solar cell's temperature, T_s is the sun's temperature, and T_0 is the emission temperature of individual cells (see [12, Eq. (10)]). For temperatures of $T_s = 6000$ (K) and $T_c = 300$ (K), the maximum efficiency is computed to be 85.4%.

[2]This efficiency was obtained by the Fraunhofer Institute for Solar Energy Systems (ISE) on September 2013 [3].

Similarly, the maximum achievable efficiency for a thermoelectric generator is

$$\eta_{\max} = \frac{T_H - T_C}{T_H} \frac{\sqrt{1 + Z(T_{\text{avg}})} - 1}{\sqrt{1 + Z(T_{\text{avg}})} + \frac{T_H}{T_C}}, \tag{1.7}$$

where T_H is the temperature of the hot junction, T_C is the temperature of cold junction, $T_{\text{avg}} = (T_H + T_C)/2$, and $Z(T_{\text{avg}})$ is the dimensionless figure-of-merit associated with ability of a material to produce thermoelectric power. In particular, $Z(T_{\text{avg}})$ is formulated as below

$$Z(T_{\text{avg}}) = \frac{\sigma S^2 T_{\text{avg}}}{\kappa}, \tag{1.8}$$

where S (V/K) is the Seebeck coefficient, $\sigma(1/\Omega\text{m})$ is electrical conductivity, and $\kappa(\text{W}/(\text{Km}))$ is thermal conductivity. Although there is no bound on $Z(T)$, the maximum reported value for $Z(T)$ is ~ 3.5 that was achieved at $T = 575$ (K) [23].

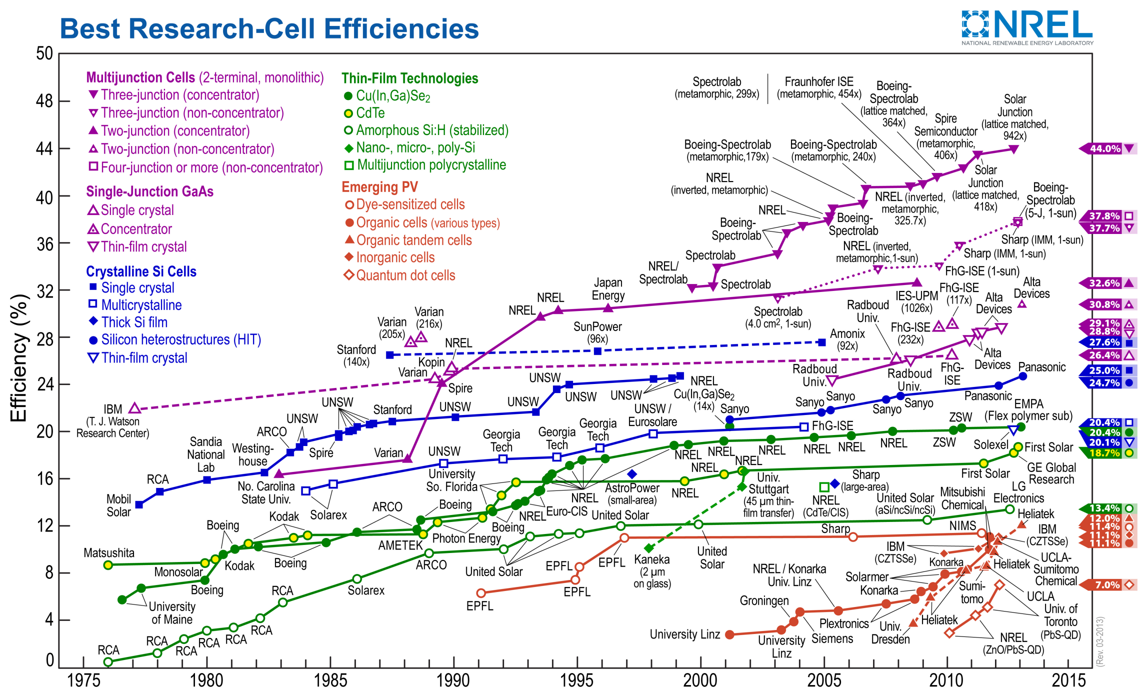

Figure 1.3: The evolution of efficiency of solar cells since 1976 (credit: US department of energy [4]).

The formulation of piezoelectric energy conversion efficiency is studied in [13]. Using a mass+spring+damper+piezo model, it was shown that the maximum efficiency in the steady state vibration regime is

$$\eta_{\max} = \frac{\frac{k_e^2}{\zeta_m}}{2\pi\Omega + \frac{k_e^2}{\zeta_m}}, \tag{1.9}$$

where the parameters are defined as

$$\zeta_m := \alpha/2\sqrt{KM}, \tag{1.10}$$
$$k_e := \Theta^2/KC_p, \tag{1.11}$$
$$\Omega := \omega/\omega_{sc}, \tag{1.12}$$

with M: the mass, K: the stiffness of spring, α: the damper's constant, Θ : the effective piezoelectric coefficienct, C_p: the piezoelectric capacitance, ω: the angular frequency of steady-state vibrations, ω_{sc}: the natural angular frequency under short-circuit. For typical values $k_e = 0.16$ and $\zeta_m = 0.03$, the maximum value of (1.9) was calculated to be 46% at $\Omega = 1$.

Table 1.2 shows a comparison between power performance of different energy harvesting techniques for wireless sensor networks.

Table 1.2: Power performance of energy harvesting methods [21].

Energy Source	**Performance**
Battery	2880 $\mathrm{J/cm^3}$
Light (indoor)	10-100 $\mu\mathrm{W/cm^2}$
Thermoelectric	40-60 $\mu\mathrm{W/cm^2}$
Piezoelectric	100-330 $\mu\mathrm{W/cm^3}$
Electromagnetic radiation	0.2-1 $\mathrm{mW/cm^2}$

1.3 Power Adaptation to EH Resources

The formulation of power policies in energy harvesting systems depends on many factors, including energy arrival model, battery capacity, quality of service, *etc.* Nevertheless, the are four main frameworks to adapt in the design of transmission powers:

1. offline or online
2. continuous time or discrete time
3. with the channel state information (CSI) or without the CSI.
4. Infinite time horizon or finite time horizon.

The first division is based on knowledge of the renewable energy resource at the transmitter. In particular, depending on causal or non-causal knowledge of future energy arrivals, power policies fall within two major categories: offline or deterministic (for non-causal), and online or stochastic (for causal).

The transmission power can also change either continuously or discretely. This depends on the coherence time of communication channel as well as the dynamic of renewable energy resources. Specifically, when the channel fading gain or the energy arrival rate fluctuates fast, a continuous transmission power must be adapted.

Furthermore, in the case that the CSI is available at the transmitter (through feedback), the power policy can be designed to dynamically allocate power to different channel states. This particularly allows the transmitter to conserve energy in bad channel states and reliably transmits with more power in good channel states.

Lastly, the time window for communication can be infinite or finite depending on different applications. The main focus of this thesis is on infinite time horizon regime. The case of finite time horizon is also addressed briefly in Appendix D.

1.4 Related Works

1.4.1 Energy Management

Energy management schemes can be classified into two main categories: 1) minimizing the radio activity 2) minimizing the number of data acquisitions by sensor.

Among the works that consider to minimize the radio activity are [17], [40], [36]. In [17], the problem of multi-hop communication in sensor networks associated with switching nodes on and off is considered. Two solutions are studied based on adaptive duty-cycling as well as wake-up on demand method. Along the same lines, a greedy algorithm to control the topology of a sensor network by tuning the transmission power of each node is studied in [40]. In [36], a wake-on-wireless strategy is proposed that increases the battery lifetime by reducing the idle power (the power consumed in standby mode).

To reduce the number of data acquisitions, a multi-scale architecture is studied in [37]. In this architecture, low-fidelity sensors first perform the measurement on the entire sensing field. Then a mobile robotic node carries high-fidelity sensors to particular spots of the field to obtain more accurate samples. In [6], adaptive sampling is proposed to dynamically estimate the optimal sampling frequency of a physical quantity to be monitored over time. In [14], a probabilistic model is derived based on a initial samples and statistical modeling techniques. This model was utilized to find certain structures (such as spatial or temporal correlation) in the sensed field. By using those structures, it was shown that the number of required samples can be reduced significantly.

1.4.2 Energy Harvesting

In the offline regime and in terms of throughput maximization, optimal power allocation for different communication topologies has been well studied. For instance, [44] studies the multiple access channel (MAC), [42] studies the broadcast channel, and the interference channel is studied in [41]. In addition, the issue of maximizing throughput in a fading channel has been treated in [31]. There, a directional water-filling algorithm is proposed. In [15], a continuous time energy harvesting system with constant energy leakage rate due to battery imperfections is considered. Another interesting problem has been studied in [43] where an offline energy harvesting problem subject to minimizing the transmission completion time is analyzed. Specifically, a continuous-time policy to minimize the delivery time of data packets is formulated. Among more recent results in the offline setting is [22] where energy cooperation in a two-hop communication system is considered.

As an overview of prior works in the online regime, we refer the reader to [31], [33], [35], and [32]. In [31] an algorithm in the offline problem of throughput maximization by a deadline was heuristically applied to the online counterpart. The authors have also considered a dynamic programming solution for online policies. Nevertheless, the curse of dimensionality in the backward induction renders the computational cost of this approach very expensive. In [33], the capacity of the additive white Gaussian noise channel (AWGN) under discrete-time energy arrivals and infinite battery capacity is characterized. Additionally, two achievable schemes based on save-and-transmit and best-effort-transmit are studied there. In [35], queuing aspects of the online energy harvesting problem with infinite battery and buffer capacity have been considered. The authors have also suggested a greedy policy that in the low signal to noise ratio (SNR) regime is throughput optimal and attains minimum delay. A more relevant study related to the work presented here is [38]. Therein, Srivastava and Koksal have investigated an optimization problem where the objective is to maximize a utility function subject to causality and battery constraints. More interestingly, they addressed a trade-off between achieving the optimum utility and keeping the discharge rate low.

1.5 Contributions

We consider the online setting with continuous time policies in which the energy release rates are regulated dynamically based on the remaining charge of the battery at each moment. This distinctive architecture naturally appeals for a different mathematical framework in terms of modelling and analysis. Particularly, the main tool here for modelling the interaction between battery, energy arrivals, and energy consumption is a stochastic process known as a *compound Poisson dam* model. This model was pioneered by Moran in 1954 [30] and studied further by Gaver-Miller [18] and Harrison-Resnick [24]. In connection with this model, we derive an upper bound on the total sum-throughput of an online energy harvesting system. Also in terms of achievability, we construct an optimization problem to maximize the sum-throughput subject to an ergodicity constraint. This maximization problem turns out to be non-linear and analytically cumbersome. Relying on a calculus of variations approach, we subsequently find a system of simultaneous PIDEs as necessary conditions for an optimal power policy. We then propose a Gauss-Seidel method (see [10]) to solve these equations efficiently. In the symmetric case, when the statistical description of all the energy harvesters are identical, we obtain an alternative algorithm using a fixed point iteration method. Moreover, in the case of the point-to-point channel setting, the necessary condition further reduces to a non-linear, autonomous ordinary differential equation (ODE) that can be solved directly, using conventional numerical methods [29].

1.6 Thesis Organization

The remainder of this thesis is organized as follows. In Chapter 2, we review some background, definitions, and notation. Furthermore, we state necessary and sufficient conditions for ergodicity of the storage process. In Chapter 3, we derive an upper bound as well as the achievability results for both finite and infinite storage cases, including two algorithms for the achievability part. These algorithms are then used to compute the numerical results. Finally, a summary of the thesis and some future outlooks are presented in Chapter 4.

Chapter 2

Online Power Policies for EH Communication over Multiple-Access Channel

2.1 Preliminaries

2.1.1 Communication model

We consider M multiple access transmission nodes that wish to transmit their data over a shared communication channel. Furthermore, each transmission node is equipped with an energy harvesting module and a battery to capture and store arriving energy packets. Throughout the paper, we denote the instantaneous transmission power at time t from the k^{th} node ($k = 1, 2, \cdots, M$) by $P_k(t)$. Also, to quantify the corresponding transmission rate of the nodes, we consider Shannon's rate function, $r(x) = \frac{1}{2}\log_2\big(1 + (x/N_0)\big)$, where N_0 denotes the noise power spectral density. In particular, Shannon's rate function carries the following properties and, unless stated otherwise, only these properties will be used in Section IV:

- [**Positivity**] $r(x) > 0$ for all $x > 0$ and $r(0) = 0$.
- [**Differentiability**] $r(x)$ is three times continuously differentiable on $x \geq 0$.
- [**Monotone increasing**] $r'(x) > 0$ for all $x \geq 0$.
- [**Concavity**] $r''(x) < 0$ for all $x \geq 0$.

Letting R_k denote the long-term average rate of the k^{th} user, we then have the rate-region described by

$$\sum_{k \in \mathcal{S}} R_k \le \lim_{T \to \infty} \frac{1}{T} \int_0^T r\left(\sum_{k \in \mathcal{S}} P_k(s)\right) ds, \tag{2.1}$$

where the inequality holds for all subsets $\mathcal{S} \subseteq \{1, 2, \cdots, M\}$, and the resulting region is a polytope called polymatroid. In this study, we restrict ourselves to the dominant face of this polymatroid (called permutahedron) that represents the total sum-throughput (or sum-rate) of the channel. Then, the sum-throughput is

$$\sum_{k=1}^{M} R_k = \lim_{T \to \infty} \frac{1}{T} \int_0^T r\left(\sum_{k=1}^{M} P_k(s)\right) ds. \tag{2.2}$$

2.1.2 Energy harvesting and storage model

In our energy harvesting model, we allow the transmission nodes to use different techniques for harnessing exogenous energy. For example, while one node may collect solar energy, another node can use a thermoelectric generator. This mechanism is especially important for sensor networks where distributed terminals may measure miscellaneous targets that also feed sensors with energy (*e.g.* see [19]). Mathematically, we assume that for each individual node $k \in \{1, 2, \cdots, M\}$, energy is replenished into the corresponding battery according to specific energy arrivals $E_k^0, E_k^1, \cdots$, where the superscript denotes the order of arrivals. Furthermore, the energy arrivals for node k are independent, identically distributed ($i.i.d$) according to $\mathbb{P}\{E_k \le x\} = B_k(x)$ which occur at random arrival times denoted by $T_k^0, T_k^1, \cdots$. The interarrival times $\Delta T_k^n = T_k^{n+1} - T_k^n$ are also assumed to be $i.i.d$ and exponentially distributed. Therefore, the attributed point process, $N_k(t) = \sum_{n \in \mathbb{N}} \mathbf{1}_{\{T_k^n < t\}}$, is a homogeneous Poisson point process with intensity denoted by λ_k. Consequently, the total energy flow $\mathcal{E}_k^{\text{In}}(0, t]$ into node k and up to time t is a compound Poisson process,

$$\mathscr{E}_k^{\text{In}}(0, t] \triangleq \sum_{i=0}^{N(t)} E_k^i. \tag{2.3}$$

To characterize the storage model, we also need to specify the output process at each transmitter. To do so, let $X_k(t)$ denote the energy stored in the k-th battery as a function of time. Then, the total energy expenditure until time t is

$$\mathscr{E}_k^{\text{Out}}(t) \triangleq \int_0^t P_k(s)\ ds, \tag{2.4}$$

$$= \int_0^t p_k(X_k(s))\ ds, \tag{2.5}$$

where $p_k(\cdot)$ represents the transmission power policy of the k-th transmitter, modulated by the available energy in the battery. Now, the storage equation in terms of the energy arrivals in (2.3) and the drift process in (2.5) is

$$X_k(t) = X_k(0) + \mathscr{E}_k^{\text{In}}(0,t] - \int_0^t p_k(X_k(s))\ ds, \tag{2.6}$$

where $x_k(0)$ is the initial (possibly random) battery reserve at time $t = 0$, and here the battery is assumed to have infinite capacity ($X_k(t) \in [0, \infty)$). In the case that the k-th battery has a finite storage capacity, say L_k, then $X_k \in [0, L_k]$, and we can similarly characterize the following dynamics,

$$X_k(t) = X_k(0) + \mathscr{E}_k^{\text{In}}(0,t] - \int_0^t p_k(X_k(s))\ ds - Z_k(t), \tag{2.7}$$

where $Z_k(t)$ is $\mathbb{R}^+$ valued process that is null at zero ($Z_k(0) = 0$), non-decreasing, continuous almost everywhere, and such that $\int_{\mathbb{R}^+}(L_k - X_k(s))\ dZ_k(s) = 0$. This process, known as reflection process [34], ensures that for any energy arrival, the storage process remains inside the boundary, *i.e.*, $X_k(t) \in [0, L_k]$.

It is also interesting to note that the application of the structures in (2.6) and (2.7) are not limited to the current problem. In fact, this formulation has wide applicability in other fields of studies. Examples include workload modulated queues [11], water reservoir dam analysis [8], food contaminants exposure in bioscience [9], *etc.* In this thesis, the ergodicity results of [8] will be used and are summarized in section III.

2.1.3 Notation

In the rest of the paper and for conciseness, we adopt several shorthand notations. In particular, $[M]$ stands for $\{1, 2, \cdots, M\}$. For $M > 1$, we define the rectangular domain $\mathcal{A}$ as

$$\mathcal{A} \triangleq [0, L_1] \times [0, L_2] \times \cdots \times [0, L_M].$$

Related to this, we also define the M dimensional integral by

$$\int_0^{L_1}\int_0^{L_2}\cdots\int_0^{L_M}(\cdot)\ dx_1dx_2\cdots dx_M,$$

which is represented by $\int_{\mathcal{A}}(\cdot)\ d\underline{x}$. For all subsets $\mathcal{S}\subseteq[M]$, we use $\mathcal{A}(\mathcal{S})$ to denote the projection of $\mathcal{A}$ onto the coordinates indexed by $\mathcal{S}$, *i.e.*,

$$\mathcal{A}(\{1,3\})=[0,L_1]\times[0,L_3].$$

Then, $\int_{\mathcal{A}(\mathcal{S})}(\cdot)\ d\underline{x}$ denotes integration over a subset of $\mathbb{R}^{|\mathcal{S}|}$. $\mathcal{A}_j$ is also a shorthand for

$$\mathcal{A}_j\triangleq[0,L_1]\cdots[0,L_{j-1}]\times[0,L_{j+1}]\cdots[0,L_M].$$

Finally, to avoid confusion between energy arrivals and the expectation operator, we use $\mathbb{E}[\cdot]$ for the latter.

2.2 Ergodic Theory of Storage Process

We here summarize necessary and sufficient conditions for ergodicity of the storage process in (2.6). Before stating the definitions regarding ergodic behaviour, we first put some mild constraints on the transmission policies. Particularly, for all $k=1,2,\cdots,M$,

1. $\forall L_k>0: 0<x_k\leq L_k\Rightarrow p_k(x_k)>0$ and $p_k(0)=0$,
2. $\forall L_k>0,\ \sup_{0<x_k\leq L_k} p_k(x_k)<\infty$.

The first condition indicates that as long as there is energy in the battery, transmission continues (otherwise, the battery would have a minimum energy reserve that can not be consumed). The second condition does not permit the energy in the battery to be consumed instantly. Regarding these constraints, we say a policy is admissible iff it fulfills these two conditions.

***Definition* 1** *The hitting time, $\tau(x)$, is defined as the first time that the energy level in the battery reaches the value of x. More specifically,*

$$\tau(x)=\inf\{t\geq 0: X(t)=x\}.$$

Definition 2 *[8, pp. 290] The storage process is said to be transient, if and only if for all initial energy levels $x(0)$ in the battery, we have $\mathbb{P}(X_t \to \infty) = 1$. Alternatively, the storage process is said to be recurrent if and only if $\mathbb{P}[\tau(x) < \infty | x(0)] = 1,\ \forall x > 0,\ x(0) \geq 0$. In the case of a recurrent storage process, it is said to be positive recurrent if it further satisfies $\mathbb{E}[\tau(x)|x(0) = x] < \infty$ for one $x > 0$ and therefore for all $x > 0$ (irreducibility). Similarly, the recurrent storage process is null recurrent if $\mathbb{E}[\tau(x)|x(0) = x] = \infty$ for one $x > 0$ and therefore for all $x > 0$.*

One motivation for surveying ergodic conditions is to rule out policies that result in transient and null recurrent battery behaviours. For example in the transient case $X(t) \to \infty$ a.s. which is unrealistic. Also, in the null recurrent case $\lim_{t\to\infty} \mathbb{P}\{X(t) \leq u | x(0) = x\} = 0, \forall x, u \geq 0$ which implies an unbounded energy reserve in the battery.

Theorem 1 *(Assmussen [8, Thm. 3.6]) The storage process $\{X_k(t)\}_{t\geq 0}$ is positive recurrent if and only if there exist a probability measure π_k that is absolutely continuous on $(0, \infty)$ and which may possess an atom at zero, $\pi_k^0 = \pi_k(\{0\})$, i.e.,*

$$\pi_k(x_k) = \pi_k^0 + \int_{0^+}^{x_k} f_k(v_k)\ dv_k, \tag{2.8}$$

and such that

$$f_k(x_k) = \frac{\lambda_k}{p_k(x_k)} \left\{ \pi_k^0 (1 - B_k(x_k)) + \int_{0^+}^{x_k} (1 - B_k(x_k - v_k)) f_k(v_k)\ dv_k \right\}. \tag{2.9}$$

Furthermore, π_k is the unique stationary distribution of the process $X_k(t)$. □

Remark 1 *The elegant proof of Assmussen for the converse part of Theorem 1 is based on an embedded Markov chain $\{X_k(n)\}$ at marked arrival times. In particular, for recurrent embedded chains, it is shown that any storage interval $(x_k^0, x_k^1), 0 < x_k^0 < x_k^1$ is recurrent in the sense of Harris. An alternative proof of the converse part of Theorem 1 adopts the additional condition $\int_0^{x_k} (1/p_k(u))\ du < \infty, \forall x_k > 0$. Due to this extra condition, the required time to reach the zero state in the absence of new arrivals from any energy level in the battery must be finite. For this constraint, it can also be shown that $x_k = 0$ is a regenerative recurrent point for the process and therefore, due to the additional constraint, the probability measure has a strict atom $\pi_k^0 > 0$ at zero.*

Remark 2 *As discussed in [8, pp. 297], in the finite energy case ($L_k < \infty$), the storage process is always positive recurrent and the probability measure is likewise governed by (2.8) and (2.9).*

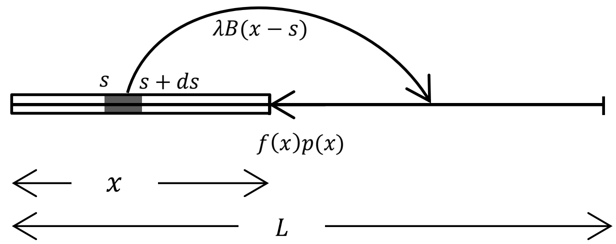

Figure 2.1: The balance between positive jumps from subspace $[0, x]$ and the drift component of the process.

Remark 3 *We note that the atom of the probability measure $\pi_k(x_k)$ corresponds to an absorbing state of the process $X_k(t)$ in the sense that upon $X_k(t)$ entering state $x_k = 0$, the process remains there until an energy arrival occurs (at which point the process transits to another state). Based on this and the first constraint on admissible power policies (in particular $p_k(L_k) > 0$), there is no atom at $x_k = L_k$ in the finite case since it has a strictly negative drift in (2.7) that shifts the process to the inner region of the state-space instantaneously, i.e., $x_k < L_k$. Therefore, the battery never idles with $x_k = L_k$ (reflecting boundary).*

An interpretation for the forward equation in (2.9) can be provided in terms of level crossing theory. Particularly,

$$f_k(x_k)p_k(x_k) = \lambda_k \left\{ \pi_k^0 \big(1 - B_k(x_k)\big) + \int_{0^+}^{x_k} \big(1 - B_k(x_k - v_k)\big) f_k(v_k)\, dv_k \right\}, \tag{2.10}$$

reflects the equilibrium condition between the rate of down crossing at level x_k (the *l.h.s* of (2.10)) and up crossing at level x_k (the *r.h.s* of (2.10)) (see Fig. 2.1) We can also view (2.9) as a Volterra integral equation of the second kind with the kernel function $\mathscr{K}(x_k, v_k) = 1 - B_k(x_k - v_k)$, and it can thus be solved numerically (see [26]).

Here, we consider the energy arrivals $\{E_k^i\}_{i=0}^{\infty}, k = 1, 2, \cdots, M$, to be exponentially distributed with parameter ζ_k. Thereby, we have

$$\mathscr{K}(x_k, v_k) = \exp(-\zeta_k(x_k - v_k)),$$

that simplifies (2.9) to

$$f_k(x_k) = \frac{\lambda_k \exp(-\zeta_k x_k)}{p_k(x_k)} G_k(x_k), \tag{2.11}$$

where

$$G_k(x_k) \triangleq \left(\pi_0 + \int_{0^+}^{x_k} \exp(\zeta_k v_k) f(v_k) \, dv_k \right). \tag{2.12}$$

Remark 4 *The storage models in (2.6) and (2.7) are memoryless, in the sense that at each time instant t, the power policy p_k only depends on the available charge $X_k(t)$ in the battery and not the entire sample path $\{X_k(s); s \leq t\}$. As an extension, we can also define a storage model with memory as follows*

$$X_k(t) = X_k(0) + \mathscr{E}_k^{\mathrm{In}}(0, t] - \int_0^t p_k(X_k(u); u \leq s) \, ds. \tag{2.13}$$

However, when the arrival process is Poisson, it can be shown that $X_k(t)$ is a sufficient statistic for an optimal power policy (see Appendix A). In this regard, knowledge of the entire path $\{X_k(s); s \leq t\}$ as an argument of $p_k(\cdot)$ is excessive.

Chapter 3

Bounds on Total Average Throughput and Achievable Schemes

3.1 Introduction

Our objective now is to derive and develop an upper bound on the average throughput as well as achievable policies with good performance. In connection with our system model, we will analyze a MAC with 1) finite, and 2) infinite storage batteries.

In particular, in the finite storage case, a good power policy must manage overflow in the battery as regular overflow causes energy waste and potentially decreases the sum throughput. To reduce overflow, the power policy must result in a large transmission power when the battery charge is large as otherwise overflow is likely to occur upon a new arrival. Nevertheless, transmitting with *too* large a transmission power when the battery happens to have large charge is also undesirable due to the concavity of the rate function. In other words, there is a tension between overflow and the rate at which the large battery charge is consumed to reduce overflow likelihood.

To further clarify the latter point, consider an energy harvesting system with a single node ($M = 1$) in which energy E is replenished into a battery exactly every T units of time. In addition, assume that the transmitter sends data by using a constant transmission power $P = E/(\alpha T), \alpha > 0$. Two cases can now be examined:

i) $\alpha > 1$: In this case, the transmitter fails to consume the entire battery charge before the next arrival, and thus overflow occurs regularly. We then have

$$T \times r\left(\frac{E}{\alpha T}\right) \leq T \times r\left(\frac{E}{T}\right). \tag{3.1}$$

ii) $\alpha < 1$: In this case, the transmitter depletes its available battery charge within $\alpha T < T$ of each arrival. From the concavity of the rate function, we have the following inequality

$$\alpha T \times r\left(\frac{E}{\alpha T}\right) \leq T \times r\left(\frac{E}{T}\right). \tag{3.2}$$

Here, the tension between (*i*) and (*ii*) is resolved by the optimal choice of $\alpha = 1$, *i.e.*, $P = E/T$.

3.2 An Upper Bound

3.2.1 Finite Storage Battery

In this case $L_k < \infty, \forall k \in [M]$. Then from (2.2) and due to ergodicity of the storage processes $\{X_k(t)_{t\geq 0}\}_{k=1}^M$ in the finite battery case (ref. Remark 3), we have almost surely

$$\sum_{k=1}^{M} R_k \stackrel{\text{a.s.}}{=} \mathbb{E}\left[r\left(\sum_{k=1}^{M} p_k(X_k)\right)\right], \tag{3.3}$$

where the expectation is with respect to the stationary distribution in Theorem 1. In addition, from the concavity property of the rate function and Jensen's inequality,

$$\mathbb{E}\left[r\left(\sum_{k=1}^{M} p_k(X_k)\right)\right] \leq r\left(\sum_{k=1}^{M} \mathbb{E}[p_k(X_k)]\right). \tag{3.4}$$

It thus remains to bound the mean transmission power $\mathbb{E}[p_k(x_k)]$. This can be accomplished by integrating by parts as follows

$$\mathbb{E}[p_k(X_k)] = \pi_k^0 p_k(0) + \int_{0^+}^{L_k} p_k(x_k) f_k(x_k)\ dx_k \tag{3.5}$$

$$\overset{(a)}{=} \int_{0^+}^{L_k} p_k(x_k) f_k(x_k)\ dx_k \tag{3.6}$$

$$\overset{(b)}{=} \lambda_k \int_{0^+}^{L_k} \exp(-\zeta_k x_k) G_k(x_k)\ dx_k \tag{3.7}$$

$$= -\frac{\lambda_k}{\zeta_k} \exp(-\zeta_k x_k) G_k(x_k)\Big|_{0^+}^{L_k} + \frac{\lambda_k}{\zeta_k} \int_{0^+}^{L_k} \exp(-\zeta_k x_k) G_k'(x_k)\ dx_k, \tag{3.8}$$

where (a) comes from the first constraint on the admissible power policies and (b) follows from (2.11). Now from (2.12),

$$G_k'(x_k) = f_k(x_k) \exp(\zeta_k x_k). \tag{3.9}$$

Also we note that $G_k(0^+) = \pi_k^0$ and

$$e^{-\zeta_k L_k} G_k(L_k) = e^{-\zeta_k L_k} \big(\pi_k^0 + \int_{0^+}^{L_k} e^{\zeta_k x_k} f_k(x_k)\ dx_k\big) \tag{3.10}$$

$$\overset{(c)}{\geq} e^{-\zeta_k L_k} \big(\pi_k^0 + \int_{0^+}^{L_k} f_k(x_k)\ dx_k\big) \tag{3.11}$$

$$= e^{-\zeta_k L_k}, \tag{3.12}$$

where inequality (c) is due to the fact that $\exp(\zeta_k x_k) \geq 1$ for all positive x_k since $\zeta_k > 0$. Substituting (3.12) and (3.9) in (3.8) thus leaves us

$$\mathbb{E}[p_k(X_k)] = \frac{\lambda_k}{\zeta_k} \big(G_k(0^+) - e^{\zeta_k L_k} G_k(L_k)\big) + \frac{\lambda_k}{\zeta_k} \int_{0^+}^{L_k} f_k(x_k)\ dx_k, \tag{3.13}$$

$$\leq \frac{\lambda_k}{\zeta_k} \big(\pi_k^0 - e^{-\zeta_k L_k} + \int_{0^+}^{L_k} f_k(x_k)\ dx_k\big) \tag{3.14}$$

$$= \frac{\lambda_k}{\zeta_k} (1 - \exp(-\zeta_k L_k)), \tag{3.15}$$

In the last step, we now use (3.15) and the non-decreasing property of the rate function to characterize an upper bound for all $L_k < \infty$ as follows

$$\sum_{k=1}^{M} R_k \leq r\Big(\sum_{k=1}^{M} \frac{\lambda_k}{\zeta_k} (1 - e^{-\zeta_k L_k})\Big) \triangleq R_{\text{upper}}. \tag{3.16}$$

3.2.2 Infinite Storage Battery

We now take $L_k = \infty$. In this case, similar to (3.7) we can directly compute,

$$\mathbb{E}[p_k(x_k)] = \lambda_k \int_{0^+}^{\infty} e^{-\zeta_k x_k} G_k(x_k)\ dx_k \tag{3.17}$$
$$= \lambda_k \int_{0^+}^{\infty} e^{-\zeta_k x_k} \Big(\pi_k^0 + \int_{0^+}^{x_k} e^{\zeta_k v_k} f_k(v_k) dv_k \Big)\ dx_k \tag{3.18}$$
$$= \frac{\lambda_k}{\zeta_k}\pi_k^0 + \lambda_k \int_{0^+}^{\infty} \int_{0^+}^{x_k} e^{\zeta_k (v_k - x_k)} f_k(v_k)\ dv_k dx_k \tag{3.19}$$
$$\stackrel{(a)}{=} \frac{\lambda_k}{\zeta_k}\pi_k^0 + \lambda_k \int_{0^+}^{\infty} \int_{v_k}^{\infty} e^{\zeta_k (v_k - x_k)} f_k(v_k)\ dx_k dv_k \tag{3.20}$$
$$= \frac{\lambda_k}{\zeta_k}\pi_k^0 + \frac{\lambda_k}{\zeta_k} \int_{0^+}^{\infty} f_k(v_k)\ dv_k \tag{3.21}$$
$$= \frac{\lambda_k}{\zeta_k}, \tag{3.22}$$

where in (a), we changed the order of integration due to the Fubini's theorem. Thus, for positive recurrent policies and when all $L_k = \infty$, we have the following upper bound

$$\sum_{k=1}^{M} R_k \le r\Big(\sum_{k=1}^{M} \frac{\lambda_k}{\zeta_k} \Big). \tag{3.23}$$

Remark 5 *In contrast with the inequality (3.16) which only holds for positive recurrent transmission power policies, (3.23) is valid for transient and null recurrent power policies as well.*

In particular, in the infinite battery case, $\lim_{T\to\infty} \frac{1}{T} \int_0^T p_k\big(X_k(t)\big)\ dt \le \lambda_k/\zeta_k$ *regardless of the type of power policy, and thus (3.23) follows by concavity of the rate function. Nevertheless, the strict equality in (3.22) will be used to study transmission power policies that result in ergodic behavior for the infinite battery capacity case in subsection 3.3.*

3.3 Achievable allocation scheme

To derive transmission power policies with good performance, we start with the ergodicity assumption and the definition of expectation, *i.e.*,

$$\sum_{k=1}^{M} R_k = \lim_{T\to\infty} \frac{1}{T} \int_0^T r\Big(\sum_{k=1}^{M} P_k(s)\Big)\ ds \tag{3.24}$$

$$\overset{\text{a.s.}}{=} \int_{\mathcal{A}} r\Big(\sum_{k=1}^{M} p_k(x_k)\Big) \prod_{k=1}^{M} \pi_k(dx_k) \tag{3.25}$$

$$\triangleq \mathcal{R}\big(\{p_k(x_k)\}_{k=1}^{M}\big), \tag{3.26}$$

where

$$\pi_k(dx_k) = [\pi_k^0 \delta(x_k) + f_k(x_k)]dx_k, \tag{3.27}$$

and $\delta(x_k)$ denotes the Dirac delta function. We now aim to find achievable policies through the following optimization problem

$$\sup_{\{\pi_k^0, f_k(x_k)\}_{k=1}^{M}} \int_{\mathcal{A}} r\Big(\sum_{k=1}^{M} p_k(x_k)\Big) \prod_{k=1}^{M} \pi_k(dx_k), \tag{3.28}$$

s.t. : $\forall k \in [M]$

$$f_k(x_k) = \frac{\lambda_k e^{-\zeta_k x}}{p_k(x_k)} \left(\pi_k^0 + \int_{0^+}^{x_k} e^{-\zeta_k v} f_k(v)\ dv\right), \tag{3.29}$$

$$\pi_k^0 + \int_{0^+}^{L_k} f_k(x_k)\ dx_k = 1, \tag{3.30}$$

$$\pi_k^0 \geq 0, \quad f_k(x_k) \geq 0, \tag{3.31}$$

which maximizes the overall expected throughput of the multiple access channel subject to the stationary probability measure constraints of the batteries. Nonetheless, tackling this non-linear optimization problem is challenging as the feasibility constraint in (3.29) is not in an explicit form. To circumvent this difficulty, we use a calculus of variations approach to transform the problem into a set of necessary conditions for an optimal solution. As a starting point, consider the following linear mappings

$$g_k(x_k) \triangleq f_k(x_k) e^{\zeta_k x_k}, \quad x_k > 0, \tag{3.32}$$

that converts the positive recurrent condition in (2.11) into

$$g_k(x_k) = \frac{\lambda_k}{p_k(x_k)}\left(\pi_k^0 + \int_{0^+}^{x_k} g_k(v)\ dv\right) \tag{3.33}$$

$$= \frac{\lambda_k}{p_k(x_k)} G_k(x_k), \tag{3.34}$$

with $G_k(x_k) = \left(\pi_k^0 + \int_{0^+}^{x_k} g_k(v)\ dv\right)$ as in (2.12). Hence, (3.25) is valid with

$$p_k(x_k) = \begin{cases} \lambda_k G_k(x_k)/g_k(x_k) & x_k > 0 \\ 0 & x_k = 0, \end{cases} \tag{3.35}$$

$$\pi_k(dx_k) = [\pi_k^0 \delta(x_k) + e^{-\zeta_k x_k} g_k(x_k)] dx_k. \tag{3.36}$$

With this substitution, we obtain an equivalent formulation for the optimization problem in (3.28)-(3.31) as below

$$\sup_{\{\pi_k^0\},\{g_k(x_k)\}} \int_{\mathcal{A}} r\Big(\sum_{k=1}^{M} p_k(x_k)\Big) \prod_{k=1}^{M} \pi_k(dx_k), \tag{3.37}$$

$$\text{s.t.} : \forall k \in [M]$$

$$G_k(x_k) = \left(\pi_k^0 + \int_{0^+}^{x_k} g_k(v)\ dv\right), \tag{3.38}$$

$$\pi_k^0 + \int_{0^+}^{L_k} e^{-\zeta_k v} g_k(v)\ dv = 1, \tag{3.39}$$

$$\pi_k^0 \geq 0, \quad g_k(x_k) \geq 0, \tag{3.40}$$

where $p_k(x_k)$ and $\pi_k(dx_k)$ are according to (3.35) and (3.36).

Through the formulation in (3.37)-(3.40), we can show that the throughput maximization problem in (3.28)-(3.31) is concave with respect to each coordinate over a convex feasible set. In particular, since the transformation between $f_k(x_k)$ and $g_k(x_k)$ is linear, the concavity of (3.28)-(3.31) can be shown equivalently by proving the concavity of the formulation in (3.37)-(3.40). To this end, suppose that $\left\{\left(\pi_k^{0,1}, g_k^1(x_k)\right)\right\}_{k=1}^M$ and $\left\{\left(\pi_k^{0,2}, g_k^2(x_k)\right)\right\}_{k=1}^M$ are two arbitrary sets of optimization parameters belonging to the feasible region defined in (3.38)-(3.40). Then for all $\alpha \in [0,1]$ and $\bar{\alpha} \triangleq (1-\alpha)$, it readily follows that $\{\left(\pi_k^{0,\alpha}, g_k^\alpha(x_k)\right)\}_{k=1}^M$ also satisfies (3.38)-(3.40), where $\pi_k^{0,\alpha} = \alpha\pi_k^{0,1} + \bar{\alpha}\pi_k^{0,2}$ and $g_k^\alpha(x_k) = \alpha g_k(x_k) + \bar{\alpha} g_k(x_k)$ are the convex combinations of the densities and atoms, respectively. This proves the convexity of the feasible region (3.38)-(3.40).

Proposition 1 *Let $\mathcal{R}_j^{\alpha}$, $\mathcal{R}_j^1$ and $\mathcal{R}_j^2$ be the utility functions corresponding to $\left\{\left(\pi_k^{0,\alpha}, g_k^{\alpha}(x_k)\right)\right\}_{k=1}^{M}$, $\left\{\left(\pi_k^{0,1}, g_k^{1}(x_k)\right)\right\}_{k=1}^{M}$, and $\left\{\left(\pi_k^{0,2}, g_k^{2}(x_k)\right)\right\}_{k=1}^{M}$ respectively, such that*

$$\begin{aligned}\left(\pi_k^{0,\alpha}, g_k^{\alpha}(x_k)\right) &= \alpha\left(\pi_k^{0,1}, g_k^{1}(x_k)\right) + \bar{\alpha}\left(\pi_k^{0,2}, g_k^{2}(x_k)\right), & k = j,\\ \left(\pi_k^{0,\alpha}, g_k^{\alpha}(x_k)\right) &= \left(\pi_k^{0,1}, g_k^{1}(x_k)\right) = \left(\pi_k^{0,2}, g_k^{2}(x_k)\right), & k \neq j.\end{aligned}$$

Then,

$$\mathcal{R}_j^{\alpha} \geq \alpha\mathcal{R}_j^1 + \bar{\alpha}\mathcal{R}_j^2. \tag{3.41}$$

Proof 2 *The proof is relegated to Appendix B.*

Now define an ensemble of perturbation functions, $\{\psi_k\}_{k=1}^{M}$, such that

$$\int_{0^+}^{L_k} \psi_k(v)\ dv = 0, \tag{3.42}$$

$$\int_{0^+}^{L_k} \exp(-\zeta_k v)\psi_k(v)\ dv = 0, \tag{3.43}$$

and the ψ_k are continuous and bounded on their domain $(0, L_k]$ with $\psi_k(0) = 0$. For sufficiently small $\epsilon_k > 0, k \in [M]$, it thus follows that $g_k^{\epsilon_k}(x_k) \triangleq g_k(x_k) + \epsilon_k\psi_k(x_k)$ meets (3.38)-(3.40) with the same atoms π_k^0 and thus lies inside the feasibility region. Then, with $\boldsymbol{\epsilon} = (\epsilon_1, \epsilon_2, \cdots, \epsilon_M)$, it must be true for a global maximum solution that

$$\mathcal{R}^{\boldsymbol{\epsilon}} \leq \mathcal{R}, \tag{3.44}$$

where

$$\mathcal{R}^{\boldsymbol{\epsilon}} = \int_{\mathcal{A}} r\Big(\sum_{k=1}^{M} p_k^{\epsilon_k}(x_k)\Big) \prod_{k=1}^{M} \pi_k^{\epsilon_k}(dx_k), \tag{3.45}$$

and

$$\begin{aligned}\pi_k^{\epsilon_k}(x_k) &\triangleq [\pi_k^0\delta(x_k) + e^{-\zeta_k x_k} g_k(x_k) + \epsilon_k e^{-\zeta_k x_k}\psi_k(x_k)]dx_k\\ &= \pi_k(dx_k) + \epsilon_k e^{-\zeta_k x_k}\psi_k(x_k)dx_k,\end{aligned} \tag{3.46}$$

and $p_k^{\epsilon_k}(x_k)$ is calculated from (3.35) to be,

$$p_k^{\epsilon_k}(x_k) = \begin{cases} \lambda_k \dfrac{G_k(x_k) + \epsilon_k \Psi_k(x_k)}{g_k(x_k) + \epsilon_k \psi_k(x_k)} & x_k > 0 \\ 0 & x_k = 0, \end{cases} \tag{3.47}$$

with,

$$\Psi_k(x_k) \triangleq \int_0^{x_k} \psi_k(v)\ dv. \tag{3.48}$$

For the moment, we assume that only the j^{th} coordinate is perturbed; that is $\epsilon_k = 0, \forall k \neq j$. Expanding the right hand side of (3.45) to first order then results in

$$\begin{aligned} \mathcal{R}^{\epsilon_j} = & \int_{\mathcal{A}} \left[r\Big(\sum_{k=1}^{M} p_k(x_k)\Big) + \epsilon_j \frac{\partial r\big(\sum_{k=1}^{M} p_k(x_k)\big)}{\partial p_j(x_j)} \frac{dp_j^{\epsilon_j}(x_j)}{d\epsilon_j}\Big|_{\epsilon_j=0} \right] \\ & \times \left[\pi_j(dx_j) + \epsilon_j e^{-\zeta_j x_j} \psi_j(x_j) dx_j \right] \prod_{k \in [M]-j} \pi_k(dx_k) \end{aligned} \tag{3.49}$$

$$\begin{aligned} = & \mathcal{R} + \epsilon_j \int_{\mathcal{A}} r\Big(\sum_{k=1}^{M} p_k(x_k)\Big) e^{\zeta_j x_j} \psi_j(x_j) dx_j \prod_{k \in [M]-j} \pi_k(dx_k) \\ & + \epsilon_j \int_{\mathcal{A}} \frac{\partial r\big(\sum_{k=1}^{M} p_k(x_k)\big)}{\partial p_j(x_j)} \frac{dp_j^{\epsilon_j}(x_j)}{d\epsilon_j}\Big|_{\epsilon_j=0} \prod_{k=1}^{M} \pi_k(dx_k) \\ & + O(\epsilon_j^2). \end{aligned} \tag{3.50}$$

On the other hand, we note that

$$\frac{dp_j^{\epsilon_j}(0)}{d\epsilon_j}\Big|_{\epsilon_j=0} = 0, \tag{3.51}$$

since $p_k^{\epsilon_j}(0) = 0$ from (3.47).[1] Therefore,

$$\int_{\mathcal{A}} \frac{\partial r\big(\sum_{k=1}^{M} p_k(x_k)\big)}{\partial p_j(x_j)} \frac{dp_j^{\epsilon_j}(x_j)}{d\epsilon_j}\Big|_{\epsilon_j=0} \delta(x_j) dx_j = 0, \tag{3.52}$$

[1] Alternatively, $p_j^{\epsilon_j}(0) = 0$ for all ϵ_j as the battery is empty.

and we thus have from (3.50)

$$\mathcal{R}^{\epsilon_j} = \mathcal{R} + \epsilon_j \int_{\mathcal{A}} r\Big(\sum_{k=1}^{M} p_k(x_k)\Big) e^{\zeta_j x_j}\psi_j(x_j)dx_j \prod_{k\in[M]-j} \pi_k(dx_k)$$
$$+ \epsilon_j \int_{\mathcal{A}} \frac{\partial r\big(\sum_{k=1}^{M} p_k(x_k)\big)}{\partial p_j(x_j)} \frac{dp_j^{\epsilon_j}(x_j)}{d\epsilon_j}\Big|_{\epsilon_j=0} e^{\zeta_j x_j} g_j(x_j)dx_j \prod_{k\in[M]-j} \pi_k(dx_k) + O(\epsilon_j^2).$$

This expansion, accompanied with inequality (3.44) establishes the following necessary condition for a locally (and thus globally) optimal solution

$$\int_{\mathcal{A}} r\Big(\sum_{k=1}^{M} p_k(x_k)\Big) e^{\zeta_j x_j}\psi_j(x_j)dx_j \prod_{k\in[M]-j} \pi_k(dx_k)$$
$$+ \int_{\mathcal{A}} \frac{\partial r\big(\sum_{k=1}^{M} p_k(x_k)\big)}{\partial p_j(x_j)} \frac{dp_j^{\epsilon_j}(x_j)}{d\epsilon_j}\Big|_{\epsilon_j=0} e^{\zeta_j x_j} g_j(x_j)dx_j \prod_{k\in[M]-j} \pi_k(dx_k) = 0, \qquad (3.53)$$

and we have neglected the second order term $O(\epsilon_j^2)$. Now with slight abuse of notation, let

$$\mathbb{E}_j\Big[r\Big(\sum_{k=1}^{M} p_k(x_k)\Big)\Big] \triangleq \int_{\mathcal{A}_j} r\Big(\sum_{k=1}^{M} p_k(x_k)\Big) \prod_{k\in[M]-j} \pi_k(dx_k), \qquad (3.54)$$

denote the expectation over all the coordinates except the j^{th}. Then (3.53) can be restated as

$$\int_0^{L_j} \Bigg[\frac{\partial \mathbb{E}_j\Big[r\big(\sum_{k=1}^{n} p_k(x_k)\big)\Big]}{\partial p_j(x_j)} \frac{dp_j^{\epsilon_j}(x_j)}{d\epsilon_j}\Big|_{\epsilon_j=0} e^{-\zeta_j x_j} g_j(x_j) + \mathbb{E}_j\Big[r\big(\sum_{k=1}^{M} p_k(z_k)\big)\Big] e^{-\zeta_j x_j}\psi_j(z_j)\Bigg]\, dx_j = 0, \qquad (3.55)$$

where we used the fact that

$$\mathbb{E}_j\left[\frac{\partial r\Big(\sum_{i=1}^{n} p_i(z_i)\Big)}{\partial p_j(z_j)}\right] = \frac{\partial}{\partial p_j(z_j)} \mathbb{E}_j\left[r\Big(\sum_{i=1}^{n} p_i(z_i)\Big)\right]. \qquad (3.56)$$

On the other hand, from (3.47), we compute

$$g_j(x_j)\frac{dp_j^{\epsilon_j}(x_j)}{d\epsilon_j}\Big|_{\epsilon_j=0} = \lambda_j\Big[\Psi_j(x_j) - \frac{\psi_j(x_j)G_j(x_j)}{g_j(x_j)}\Big] \qquad (3.57)$$
$$= \lambda_j\Psi_j(x_j) - \psi_j(x_j)p_j(x_j). \qquad (3.58)$$

We thus further proceed by substituting (3.58) in (3.55), *i.e.*,

$$\int_0^{L_j} \Big[\lambda_j e^{-\zeta_j x_j} \frac{\partial \mathbb{E}_j\big[r\big(\sum_{k=1}^M p_k(x_k)\big)\big]}{\partial p_j(x_j)}\Big] \Psi_j(x_j) dx_j$$
$$- \int_0^{L_j} \Big[e^{-\zeta_j x_j} \frac{\partial \mathbb{E}_j\big[r\big(\sum_{k=1}^M p_k(x_k)\big)\big]}{\partial p_j(x_j)} p_j(x_j) + e^{-\zeta_j x_j} \mathbb{E}_j\big[r\big(\sum_{k=1}^M p_k(x_k)\big)\big]\Big] \psi_j(x_j)\ dx_j = 0. \tag{3.59}$$

Integrating by parts, the second integral can be evaluated as follows

$$\int_0^{L_j} \Big[e^{-\zeta_j x_j} \frac{\partial \mathbb{E}_j\big[r\big(\sum_{k=1}^n p_k(x_k)\big)\big]}{\partial p_j(x_j)} p_j(x_j) + e^{-\zeta_j x_j} \mathbb{E}_j\big[r\big(\sum_{k=1}^M p_k(x_k)\big)\big]\Big] \psi_j(x_j)\ dx_j$$
$$= \Big[e^{-\zeta_j x_j} \frac{\partial \mathbb{E}_j\big[r\big(\sum_{k=1}^M p_k(x_k)\big)\big]}{\partial p_j(x_j)} p_j(x_j) + e^{-\zeta_j x_j} \mathbb{E}_j\big[r\big(\sum_{k=1}^M p_k(x_k)\big)\big]\Big] \Psi_j(x_j)\Big|_0^{L_j}$$
$$+ \int_0^{L_j} \frac{\partial}{\partial x_j}\Big[e^{-\zeta_j x_j} \frac{\partial \mathbb{E}_j\big[r\big(\sum_{k=1}^M p_k(x_k)\big)\big]}{\partial p_j(x_j)} p_j(x_j) + e^{-\zeta_j x_j} \mathbb{E}_j\big[r\big(\sum_{k=1}^M p_k(x_k)\big)\big]\Big] \Psi_j(z_j)\ dx_j. \tag{3.60}$$

But since $\Psi_j(0) = \Psi_j(L_j) = 0$ due to the definition in (3.48) and (3.42), the second term in (3.60) vanishes. Replacing the remaining terms in (3.59), then

$$\int_0^{L_j} \Bigg(\lambda_j e^{-\zeta_j x_j} \frac{\partial \mathbb{E}_j\big[r\big(\sum_{k=1}^M p_k(x_k)\big)\big]}{\partial p_j(x_j)} - \frac{\partial}{\partial x_j}\Big[e^{-\zeta_j x_j} \frac{\partial \mathbb{E}_j\big[r\big(\sum_{k=1}^M p_k(x_k)\big)\big]}{\partial p_j(x_j)} p_j(x_j)$$
$$+ e^{-\zeta_j x_j} \mathbb{E}_j\big[r\big(\sum_{k=1}^M p_k(z_k)\big)\big]\Big]\Bigg) \Psi_j(x_j) dx_j = 0, \tag{3.61}$$

which must remain valid for all $\Psi_j(x_j)$ such that $\Psi_j(x_j)$ satisfies (3.42) and (3.43). A family of solutions for equation (3.61) can be supplied by simultaneously noting from (3.43) that

$$0 = \int_0^{L_j} e^{-\zeta_j x_j} \psi_j(x_j)\ dx_j \tag{3.62}$$

$$= e^{-\zeta_j x_j} \Psi_j(x_j)\Big|_0^{L_j} + \zeta_j \int_0^{L_j} e^{-\zeta_j x_j} \Psi_j(x_j)\ dx_j \tag{3.63}$$

$$\overset{(a)}{=} \zeta_j \int_0^{L_j} e^{-\zeta_j x_j} \Psi_j(x_j)\ dx_j, \tag{3.64}$$

where (a) is true since $\Psi_j(0) = \Psi_j(L_j) = 0$ as noted before. Now, if $p_j(x_j)$ is twice continuously differentiable, it follows that the term inside the parentheses in (3.61) is continuously differentiable as the rate function $r(x)$ is assumed to be three times continuously differentiable. Furthermore, since $\psi_j(x_j)$ is also continuously differentiable, from (3.64) and the fundamental lemma of the calculus of variations, we subsequently conclude that (3.61) holds only if the term inside the parentheses is in the form of $K_j \exp(-\zeta_j x_j)$ for some constant K_j. Thus, as a necessary condition, we have

$$p_j(x_j)p_j'(x_j)\frac{\partial^2 \mathbb{E}_j[r(\sum_{k=1}^M p_k(x_k))]}{\partial^2 p_j(x_j)} + (\lambda_j - \zeta_j p_j(x_j)) \times \frac{\partial \mathbb{E}_j[r(\sum_{k=1}^M p_k(x_k))]}{\partial p_j(x_j)} + \zeta_j \mathbb{E}_j[r(\sum_{k=1}^M p_k(x_k))] + K_j = 0. \tag{3.65}$$

Remark 6 *Rewriting* (3.65) *as*

$$p_j'(x_j) = \left[- p_j(x_j)\frac{\partial^2 \mathbb{E}_j[r(\sum_{k=1}^M p_k(x_k))]}{\partial^2 p_j(x_j)}\right]^{-1}\Big[(\lambda_j - \zeta_j p_j(x_j)) \times \frac{\partial \mathbb{E}_j[r(\sum_{k=1}^M p_k(x_k))]}{\partial p_j(x_j)} + \zeta_j \mathbb{E}_j[r(\sum_{k=1}^M p_k(x_k))] + K_j\Big], \tag{3.66}$$

it is easy to verify that K_j provides a degree of freedom to set the initial slope $p_j'(x_j)\big|_{x_j=0^+}$ of the power policy $p_j(x_j)$.

Now since the choice of j^{th} coordinate was arbitrary, (3.65) holds for all $j \in [M]$. Accordingly, we obtain a system of coupled PIEDs over M coordinates with $2M$ degree of freedoms where the integration is implicit in the notation of $\mathbb{E}_j[\cdot]$ (ref. Eq. (3.54)).[2] In the following, we consider solutions in the infinite and finite battery cases.

[2]In the system of equations, $\{p_k(0^+)\}_{k=1}^M$ and $\{p_k'(0^+)\}_{k=1}^M$ (or equivalently $\{p_k(0^+)\}_{k=1}^M$ and $\{K_k\}_{k=1}^M$) are free parameters.

3.3.1 Infinite Storage Battery

Motivated by the converse result for the infinite storage battery, we consider a set of admissible policies as below

$$\bar{p}_k(x_k) = \begin{cases} \big(\lambda_k/\zeta_k\big) + \varrho & x_k > 0 \\ 0 & x_k = 0, \end{cases} \tag{3.67}$$

where the excess power $\varrho > 0$ is added to ensure the positive recurrence of the process. In the limit, as $\varrho \to 0$, the suggested policies in (3.67) satisfy (3.65) for all j, provided

$$K_j = -\zeta_j \mathbb{E}_j \left[r\big(\sum_{k=1}^{M} \frac{\lambda_k}{\zeta_k} \big) \right]. \tag{3.68}$$

The average transmission power of (3.67) can then be evaluated as

$$\mathbb{E}[\bar{p}_k(x_k)] = \pi_k^0 \bar{p}_k(0) + \big((\lambda_k/\zeta_k) + \varrho\big) \int_{0^+}^{\infty} f_k(x_k) dx_k \tag{3.69}$$

$$= \big((\lambda_k/\zeta_k) + \varrho\big)\big(1 - \pi_k^0\big) \tag{3.70}$$

On the other hand, in light of (3.22) we have $\mathbb{E}[\bar{p}_k(x_k)] = \lambda_k/\zeta_k$. As a result, a transmission node that exploits $\bar{p}_k(x_k)$ as transmission power policy has the following probability mass at zero

$$\pi_k^0 = \frac{\varrho}{(\lambda_k/\zeta_k) + \varrho}, \tag{3.71}$$

i.e., it sends information for a fraction $\dfrac{(\lambda_k/\zeta_k)}{\varrho + (\lambda_k/\zeta_k)}$ of time. Moreover, associated with $\bar{p}_k(x_k)$, the mean square deviation of transmission power is given by

$$\sigma^2\big(\bar{p}_k(X_k)\big) = \big(\frac{\lambda_k}{\zeta_k}\big)^2 \pi_k^0 + \int_{0^+}^{\infty} \Big(\bar{p}_k(x_k) - \frac{\lambda_k}{\zeta_k}\Big)^2 f_k(x_k)\, dx_k \tag{3.72}$$

$$= (\lambda_k/\zeta_k)\varrho. \tag{3.73}$$

For these power transmission strategies, we also have

$$\mathcal{R} \geq r\Big(\sum_{k=1}^{M} (\lambda_k/\zeta_k + \varrho) \Big) \prod_{k=1}^{M} \frac{(\lambda_k/\zeta_k)}{(\lambda_k/\zeta_k) + \varrho}, \tag{3.74}$$

where the inequality follows from neglecting situations in which a strict subset of nodes are transmitting and the rest are silent due to battery exhaustion. As $\varrho \downarrow 0$, the upper bound (3.23) and the lower bound (3.74) coincide with each other. The total average throughput is given asymptotically by

$$\mathcal{R} = r\Big(\sum_{k=1}^{M} \lambda_k/\zeta_k\Big). \tag{3.75}$$

Thus, near optimal performance of the energy harvesting system can be achieved when $\varrho \downarrow 0$, and the behaviour of a classical communication systems (in the sense of using a constant power supply without interruption) can be closely approximated at the same time.

3.3.2 Finite Storage Battery

In contrast to the case of batteries with infinite capacity, the system of equations in (3.65) doesn't appear to admit a closed form expression for power policies when the storage capacity is finite. The remaining option is thus to solve (3.65) numerically. However, the complexity in dealing with such systems is that the equations are not independent, but *coupled*. Alternatively, if all but one of the $p_k(\cdot)$ are known, the remaining one can be obtained by solving a first order non-linear ODE in terms of the corresponding coordinate, using (3.65). First from (3.34) and since $G'_k(x_k) = g_k(x_k)$ we obtain by integration

$$\ln G_k(x_k) - \ln G_k(0) = \int_{0^+}^{x_k} \frac{\lambda_k}{p_k(v_k)}\, dv_k. \tag{3.76}$$

Therefore,

$$G_k(x_k) = \pi_k^0 \exp\Big(\int_{0^+}^{x_k} \frac{\lambda_k}{p_k(v)}\, dv\Big). \tag{3.77}$$

By differentiating both sides with respect to x_k, we obtain

$$g_k(x_k) = \frac{\pi_k^0 \lambda_k}{p_k(x_k)} \exp\Big(\int_{0^+}^{x_k} \frac{\lambda_k}{p_k(v)}\, dv\Big), \tag{3.78}$$

or equivalently,

$$f_k(x_k) = \pi_k^0 \frac{e^{-\lambda_k x_k}\lambda_k}{p_k(x_k)} \exp\Big(\int_{0^+}^{x_k} \frac{\lambda_k}{p_k(v)}\, dv\Big). \tag{3.79}$$

Also due to the normalization condition

$$\pi_k^0 + \int_{0^+}^{L_k} f_k(x_k)\ dx_k = 1, \tag{3.80}$$

we have

$$\pi_k^0 = \left[1 + \int_{0^+}^{L_k} \frac{e^{-\lambda_k x_k}\lambda_k}{p_k(x_k)} \exp\Big(\int_{0^+}^{x_k} \frac{\lambda_k}{p_k(v)}\ dv\Big) dx_k\right]^{-1}, \tag{3.81}$$

which can simply be derived via substituting (3.79) in (3.80) and solving for π_k^0.

With the help of (3.79) and (3.81), we propose an iterative method, outlined as Algorithm 1, that computes a solution for (3.65). Also, the convergence analysis of Algorithm 1 follows three steps

i) at each iteration of Algorithm 1, the utility function (3.25) is non-decreasing,

ii) the utility function in (3.25) is bounded above,

iii) the utility (3.25) thus converges if Algorithm 1 is allowed to iterate indefinitely (*i.e.* no termination constraint).

Specifically, in the first step, we denote the utility $\mathcal{R}$ as an explicit function of the power policies in Algorithm 1, *e.g.*, $\mathcal{R}(p_1^{(0)}(x_1), p_2^{(0)}(x_2), \cdots, p_M^{(0)}(x_M))$ is the initial utility. After the Nth full iteration of steps 5-10 (outer loop) of Algorithm 1, in the jth iteration of 6-10 (inner loop), we then obtain

$$p_j^{(N+1)}(x_j) = \arg\max_{\xi} \mathcal{R}(p_1^{(N+1)}(x_1), \cdots, p_{j-1}^{(N+1)}(x_{j-1}), \xi, p_{j+1}^{(N)}(x_{j+1}), \cdots, p_M^{(N)}(x_M)).$$

Therefore,

$$\mathcal{R}(p_1^{(N+1)}(x_1), \cdots, p_j^{(N)}(x_j), \cdots, p_M^{(N)}(x_M)) \leq \mathcal{R}(p_1^{(N+1)}(x_1), \cdots, p_j^{(N+1)}(x_j), \cdots, p_M^{(N)}(x_M)). \tag{3.82}$$

In addition, since the objective function is upper bounded by (3.16), we further have

$$\mathcal{R}_{\text{sup}} \triangleq \sup_{\{p_k(x_k)\}} \mathcal{R}(p_1(x_1), p_2(x_2), \cdots, p_M(x_M)) \tag{3.83}$$

$$\leq r\Big(\sum_{k=1}^{M} \frac{\lambda_k}{\zeta_k}(1 - \exp(-\zeta_k L_k))\Big). \tag{3.84}$$

Algorithm 1

for all $k \in [M]$ **do**
  initialize $p_k(x_k)$ with some arbitrary function;
  compute (3.79) and (3.81);
end for
repeat
  for $j \leftarrow 1, M$ **do**
    calculate (3.54);
    update $p_j(x_j)$ by solving (3.65) for optimized values of $p_j(0^+)$ and K_j;
    update (3.79) and (3.81) for $k = j$;
  end for
until termination criterion is satisfied.

Concluding from (3.82) and (3.84), the sequence $\mathcal{R}\big(\{p_k^N(x_k)\}_{N=0}^{\infty}\big)$ must converge in the limit as $N \to \infty$.

Now, we concentrate on two important degenerate cases of our problem that can substantially reduce the computational burden of solving the PIEDs. In the first scenario, suppose that all the transmission nodes scavenge energy in the same manner. By this statement, we mean that the statistical parameters of all the energy harvesters are identical, *i.e.*, $\lambda_k = \lambda$ and $\zeta_k = \zeta$ for all $k = 1, 2, \cdots, M$. In the symmetric case, further assume that the batteries have identical capacities ($L_k = L$). These assumptions then let us apply one policy to all the transmitters ($p_k(x_k) = p(x_k)$) and to specialize (3.65) as below

$$\begin{aligned} p(x_j)p'(x_j)\frac{\partial^2 \mathbb{E}_j[r(\sum_{k=1}^M p(x_k))]}{\partial^2 p(x_j)} &+ (\lambda - \zeta p(x_j)) \\ \times \frac{\partial \mathbb{E}_j[r(\sum_{k=1}^M p(x_j))]}{\partial p(x_j)} &+ \zeta \mathbb{E}_j[r(\sum_{k=1}^M p(x_j))] + K = 0, \end{aligned} \tag{3.85}$$

where j is arbitrary and chosen from $[M]$, and the operator $\mathbb{E}_j[\cdot]$ now simplifies as

$$\mathbb{E}_j\left[r\Big(\sum_{k=1}^M p(x_k)\Big)\right] = \int_{\mathcal{A}_j} r\Big(\sum_{k=1}^M p(x_k)\Big) \prod_{k\in[M]-j} \pi(dx_k). \tag{3.86}$$

If we rearrange the terms in equation (3.85), we have that

$$p(x_j) = \mathscr{F}\big(p(x_j)\big), \tag{3.87}$$

where the mapping $\mathscr{F}(\cdot):\mathbb{C}^1(0,L]\to\mathbb{C}^1(0,L]$ is given by

$$\mathscr{F}\big(p(x_j)\big) = p(0^+) - \int_{0^+}^{x_j} \Big[K_j + \zeta\mathbb{E}_j[r(\sum_{k=1}^{M} p(v_k))] + (\lambda-\zeta p(v_j)) \times \frac{\partial\mathbb{E}_j[r(\sum_{k=1}^{M} p(v_k))]}{\partial p(v_j)}\Big]\Big[p(v_j)\frac{\partial^2\mathbb{E}_j[r(\sum_{k=1}^{M} p(v_k))]}{\partial^2 p(v_j)}\Big]^{-1} dv_j. \tag{3.88}$$

As a result, it follows that the desired $p(x_j)$ is a fixed point for $\mathscr{F}(\cdot)$. This then supplies us with an alternative algorithm for this special case (see Algorithm 2).

Now in the second scenario, consider that there is only one transmitter in the communication system (*i.e.* a point-to-point setup). We thus have a simplified formulation as a necessary condition here, *i.e.*,

$$p(x)p'(x)\frac{d^2r\big(p(x)\big)}{d^2p(x)} + \big(\lambda-\zeta p(x)\big)\frac{dr\big(p(x)\big)}{dp(x)} + \zeta r\big(p(x)\big) + K = 0. \tag{3.89}$$

As argued in [29], this is a second order, non-linear, autonomous ODE that can be solved numerically by employing linear multistep methods (*e.g.* Runge-Kutta or Adams-Bashforth). The next lemma demonstrates some properties of solutions to this ODE.

***Lemma* 1** *Suppose $K > -\zeta r(\lambda/\zeta)$ in (3.89), then for the Shannon rate function*

(a) any solution $p(x)$ is a strictly increasing function of x for $x \geq 0$, and $p(x)\to\infty$ as $x\to\infty$.

(b) $p(x)$ grows doubly exponentially fast as $x\to\infty$. □

***Proof* 3** *Solving (3.89) for $p'(x)$, we have*

$$p'(x) = \frac{\big(\lambda-\zeta p(x)\big)r'\big(p(x)\big) + \zeta r\big(p(x)\big) + K}{-p(x)r''\big(p(x)\big)}. \tag{3.90}$$

From concavity of the rate function as well as the first constraint on admissible power policies we have $r''(p(x)) < 0$ and $p(x) \geq 0$, respectively. Therefore, the denominator is always positive and $p'(x) > 0$ for all $x \geq 0$ iff

$$K > -\big[\big(\lambda-\zeta p(x)\big)r'\big(p(x)\big) + \zeta r\big(p(x)\big)\big], \quad \forall x > 0. \tag{3.91}$$

Algorithm 2

1: initialize $p^{(0)}(x_j)$ with some function.
2: **repeat**
3: compute (3.79) and (3.81);
4: compute (3.86);
5: update $p^{(N+1)}(x_j) = \mathscr{F}(p^{(N)}(x_j))$ from (3.88) for optimized values of $p^{(N)}(0^+)$ and $K^{(N)}$;
6: **until** termination criterion is satisfied.

Moreover, it can be verified that

$$\frac{d}{dp(x)}\left[\big(\lambda - \zeta p(x)\big)r'\big(p(x)\big) + \zeta r\big(p(x)\big)\right] = \big(\lambda - \zeta p(x)\big)r''(p(x)).$$

Hence, $p(x) = \lambda/\zeta$ is a global maxima for the right hand side of (3.91). Replacing $p(x) = \lambda/\zeta$ into (3.91), the numerator of (3.90) is then lower bounded by

$$K + \zeta r(\lambda/\zeta) > 0.$$

Furthermore, since $r(x) = \frac{1}{2}\log_2(1 + \frac{x}{N_0})$, we upper bound the denominator by

$$\begin{aligned}
-p(x)r''(p(x)) &= \frac{1/N_0}{2\ln 2}\frac{p(x)/N_0}{(1 + p(x)/N_0)^2} \\
&\leq \frac{1/N_0}{8\ln 2}.
\end{aligned}$$

and thus $p(x) \to +\infty$.

To prove the second part of Lemma 1, consider the substitution

$$p(x)/N_0 = \exp(S(x)), \tag{3.92}$$

where $S(x)$ increases since $p(x)$ increases. Then we have

$$S(x) \to +\infty, \quad \text{as } x \to \infty. \tag{3.93}$$

Consequently, for the Shannon rate function we obtain

$$\frac{dr\big(p(x)\big)}{dp(x)} = \frac{1}{2\ln 2}\frac{1/N_0}{1 + p(x)/N_0} \simeq \frac{1/N_0}{2\ln 2}\exp(-S(x)), \tag{3.94}$$

$$\frac{d^2r\big(p(x)\big)}{dp(x)^2} = \frac{-1}{2\ln 2}\frac{1/N_0^2}{(1 + p(x)/N_0)^2} \simeq \frac{-1/N_0^2}{2\ln 2}\exp(-2S(x)), \tag{3.95}$$

and

$$r(p(x)) = \frac{1}{2}\log_2\big(1 + p(x)/N_0\big) \simeq \frac{1}{2\ln 2}S(x). \tag{3.96}$$

Replacing (3.94)-(3.96) in (3.89) yields that for $x \to \infty$

$$-S'(x) + (\lambda - \zeta N_0 e^{S(x)})(e^{-S(x)}/N_0) + \zeta S(x) + (K/2\ln 2) = 0, \tag{3.97}$$

As $x \to \infty$ and due to (3.93), (3.97) reduces to

$$\zeta S(x) = S'(x), \tag{3.98}$$

which has the following solution

$$S(x) = A\exp(\zeta x), \tag{3.99}$$

for some constant A, and thus

$$p(x) = O\big(\exp(e^{\zeta x})\big), \;\; \textit{as } x \to \infty. \tag{3.100}$$

Remark 7 *On account of Lemma 1, it is easy to verify that when $K \leq -\zeta r(\lambda/\zeta)$, the property of (3.100) does not hold in general. In fact, for sufficiently large negative K, solutions of (3.89) are decreasing power policies. However, we conjecture that all such power policies are suboptimal as they fail to control the overflow in the battery. A more detailed discussion will be presented in the following section.*

3.4 Discussion and Numerical Solution

We now study a multiple access communication system consisting of two nodes ($M = 2$) with $\lambda_1 = \lambda_2 = \lambda = 1$ and $\zeta_1 = \zeta_2 = \zeta = 1$. Because of the symmetry of the MAC, the achievable power policies for this setting are obtained through Algorithm 2. Nevertheless, to implement Algorithm 2 according to steps 1-6, one is obliged to search for optimized values of $p(0^+)$ and K at each iteration. To ease this process and in what follows, Algorithm 2 is modified in a way that once the values of $p(0^+)$ and K are initialized, the same values are used at each iteration step. [3]

[3]Although this approach is potentially suboptimal, it always yields achievable results, and in the case of the considered example here, the achievable results are close to the upper bound.

Table 3.1:
Total average throughput for two identical nodes, using Shannon rate function, $r(x) = \frac{1}{2}\log(1 + x/N_0)$, with $N_0 = 1$, equation constant $K = 0$, initializing function $p^{(0)}(x) = x + p(0^+), 0 < x \leq L$, and for various storage capacity L and initial values $p(0^+)$.

		Initial Value $p(0^+)$			
L	R_{upper}	0.001	0.001	0.1	1
0.5	0.4187	0.3177	0.3152	0.3094	0.2797
1	0.5895	0.4217	0.4159	0.4069	0.3722
2	0.7243	0.4634	0.4575	0.4511	0.4075
3	0.7681	0.4652	0.4593	0.4510	0.4091

With this modification, Fig. 3.1a then illustrates the designed power policy as a function of the remaining charge in the battery with initial conditions $p(0^+) = 0.1$ and $K = 0$ and initializing function $p^{(0)}(x_k) = x_k + p(0^+), 0 \leq x_k \leq L_k$. After $N = 10$ iterations, the power policy has converged to a solution of (3.85). It can also be seen from Fig. 3.1a that as the remaining charge in the battery increases, the transmission power also increases rapidly. Supported by part (b) of Lemma 1, we further conjecture that this increase is in fact doubly exponential in x. Indeed, when the occupied charge of the battery becomes large, the chance of overflow due to new energy arrivals increases as well. In this regard, an optimal power policy is one which consumes the battery charge fast enough such that the occurrence of overflow is traded-off against suboptimality of employing a large instantaneous transmission power (see Section IV). On the other hand, for sufficiently large negative K, solutions of (3.85) are non-increasing (ref. Remark 7 for the point-to-point case) and they thus fail to manage battery overflow. The numerical results have further verified that for non-increasing power policies, the achieved sum-throughput is strictly less than for increasing ones. As a result, here we only consider increasing power policies.

Corresponding to the designed power policy in Fig. 3.1a, Fig. 3.1b shows the absolutely continuous part (density) of the probability measure in (2.8). In this case, consistent with our earlier observation for the power policy, the density function also falls off quickly. In terms of ergodicity, this is basically an assertion of the fact that the system spend little time with large stored charge in the battery. Using Algorithm 2, we have computed the achievable rates provided in Table I and Table II, where the termination criterion is taken to be

$$\theta = \frac{r\left(\sum_{k=1}^{M} p^{N+1}(x_k)\right) - r\left(\sum_{k=1}^{M} p^{N}(x_k)\right)}{r\left(\sum_{k=1}^{M} p^{N}(x_k)\right)} < 1\%,$$

Table 3.2:
Total average throughput for two identical nodes, using Shannon rate function, $r(x) = \frac{1}{2}\log(1+x/N_0)$, with $N_0 = 1$, initial value $p(0^+) = 0.001$, initializing function $p^{(0)}(x) = x + p(0^+), 0 < x \leq L$, and for various storage capacity L and equation constant K. The upper bound for an infinite storage battery ($L_k = \infty$) is given by $R_\infty = \frac{1}{2}\log(1+2) = 0.792$.

		Equation Constant K			
L	R_{upper}	$+0.5$	0	-0.5	Optimum(% of R_{upper})
0.5	0.4187	0.3017	0.3177	0.3057	0.3262 (77.9%) [K=-0.15]
1	0.5895	0.3707	0.4217	0.4410	0.4612 (78.2%) [K=-0.37]
2	0.7243	0.3854	0.4634	0.5725	0.5951 (82.1%) [K=-0.63]
3	0.7681	0.3858	0.4652	0.5907	0.6654 (86.6%) [K=-0.67]

i.e., the iteration stops whenever the increase in rate is less than one percent. With this precision, Table 3.1 shows the sum throughput for several choices of $p(0^+)$ and fixed $K = 0$. The upper bound is also computed from (3.16) and denoted by R_{upper} in the table.

Based on a comparison between the upper and lower limits on the rate function, it is immediate that the choice of $p(0^+) = 0.001$ results the best performance of the designed power policy. For the same choices of $p(0^+)$ as in Table 3.1 and $K = 0$, Fig. 3.2 shows the power policy solutions. Except for the case of $p(0^+) = 1$, all the power policy solutions adopt a small transmission power when battery charge is small. Along the same lines, Table 3.2 shows the upper and lower limits on the average throughput for fixed $p(0^+) = 0.001$ and variable K. We have particularly provided the best value of K up to precision 0.01 as well as the corresponding achievable rates. The best achievable rate, as a percentage of the *upper bound*, is also evaluated.

Finally, to show the robustness of the iterative algorithm to the initializing function, a different choice of $p_k^{(0)}(x_k)$ is studied in Fig. 3.3. Therein, we particularly have selected $p_k^{(0)}(x_k) = p_k(0^+), 0 \leq x_k \leq 3$ for purpose of initialization in Algorithm 2 while the rest of the parameters are the same as in Fig. 1a. Evidently, the power policy converges to an identical function as one depicted in Fig. 1a. Similarly, the same convergence was observed when $p_k^{(0)}(x_k) = p_k(0^+) + \sqrt{x_k}, 0 \leq x_k \leq 3$. In this respect, the proposed algorithm appears to be insensitive to the choice of the initial power policy.

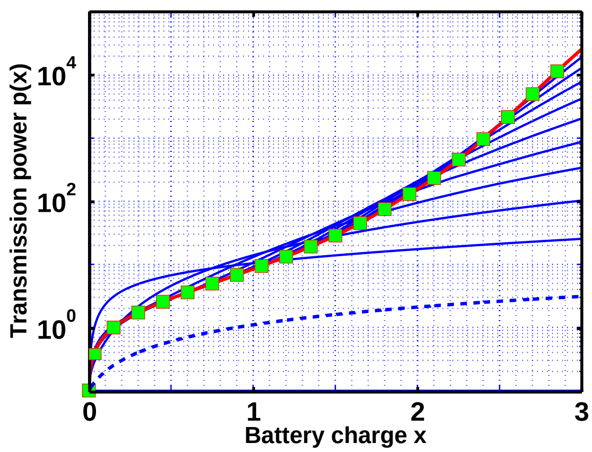

(a)

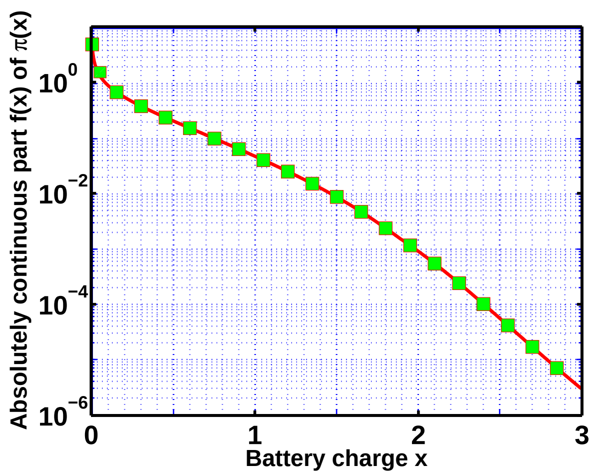

(b)

Figure 3.1: Battery capacity $L = 3$, equation constant $K = 0$, and $p(0^+) = 0.1$ for two nodes case. (a) The convergence of transmission power policy to an achievable policy (denoted by squares) after $N = 10$ iterations with initializing function $p^{(0)}(x) = x + p(0^+)$ (dashed lines) and iterates (solid lines), (b) Absolutely continuous part $f(x)$ of $\pi(x)$ for the converged solution.

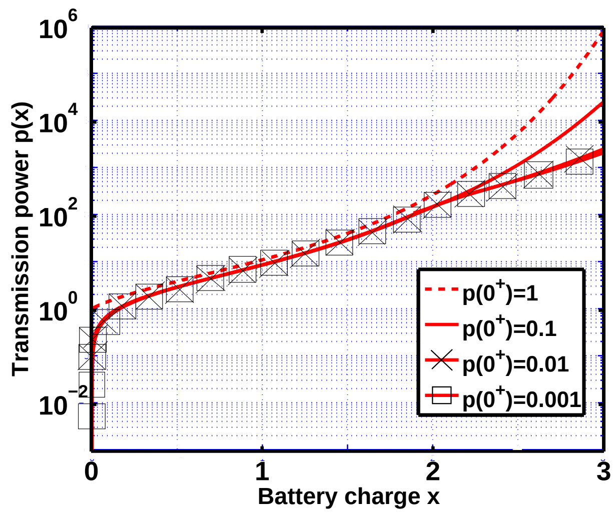

Figure 3.2: Transmission power policies $p(x)$ with different initial values $(L = 3, M = 2, K = 0)$.

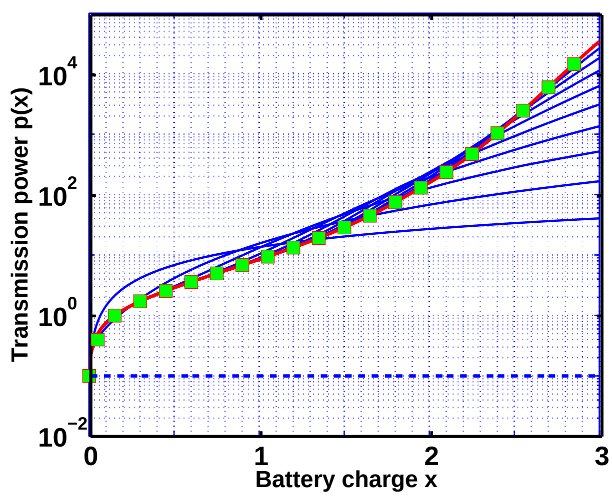

Figure 3.3: Robustness to the initializing function, using a constant initializing function (dashed line) $p^{(0)}(x_k) = p(0^+), 0 \leq x_k \leq L$ $(L = 3, M = 2, K = 0$ and $N = 10)$.

Chapter 4

Summary and Future Research

4.1 Summary

We have considered continuous-time power policies for a multiple access communication system where each node is capable of harvesting energy.

First, we modelled the battery as a compound Poisson dam, where the remaining charge in the battery modulates the transmission power. We then analysed this storage dam model in the ergodic case. In particular, we characterized an upper bound on the maximum sum-rate as a function of the energy arrivals distributions and the capacity of the batteries.

For batteries with infinite capacity, we proved that any rate close to the upper bound is achievable by a set of constant power policies. For batteries with limited capacity, we showed that optimal power policies can be derived by solving a system of simultaneous partial integro-differential equations. To solve these equations, we developed an iterative algorithm based on the Gauss-Seidel approach.

We next derived a fixed point algorithm for the symmetric MAC case where the multiple access nodes have identical energy harvesting statistics. Furthermore, the convergence of the utility function that results from the proposed algorithms was established. Numerical results show that for a battery capacity of $L = 3$, the achievable scheme provides a throughput of up to 86.6% of the upper bound.

4.2 Future Research and Extensions

Clearly, the problem is still open in the finite battery case due to the gap that exists between the given upper bound and achievable rates. Therefore, further investigation is required to close the gap by obtaining a tighter upper bound or better achievable power allocation schemes.

An interesting extension to this work is to study energy harvesting communication over fading channels, where the transmission power is adapted to both channel fading process and storage process of battery. This study particularly reveals the relation between the water-filling power policy (for a constant average power constrain) and energy harvesting power policies.

Another extension is to consider continuous-time power policies that are modulated by the stored energy and data in the battery and buffer, respectively. In this case, the performance metric can be either the average transmission rate or the average delay incurred by data packages in the buffer. Furthermore, based on a generalized rate conservation law for multi-dimensional càdlàg processes (see [20]), necessary conditions for ergodicity of the energy storage process can be established.

Current and Future direction in energy harvesting technologies is concentrated on the fabrication of hybrid EH devices where different energy sources can be harvested in one platform. Therefore, the power output of EH devices is expected to substantially increase in the near future. The energy harvesting technologies will thus play a central role in the global power supply chain over the next decades.

APPENDICES

Appendix A

Optimality of Markov Power Policies

In the following, we show that for every power policy with memory, $p_k^*(X_k(u); u \leq t)$, there exist a memoryless counterpart $p_k(X_k(t))$ that attains the same or better sum-throughput performance. In particular, let $(\Omega, \mathcal{F}, \mathbb{P})$ be a complete probability space and $X_k^*(t;\omega), -\infty < t < \infty$ be a stationary and ergodic stochastic process defined on this probability space and whose evolution for $t \geq 0$ is given by[1]

$$X_k^*(t;\omega) = X_k^*(0;\omega) + \mathscr{E}_k^{\mathrm{In}}\big((0,t];\omega\big) - \int_0^t p_k^*\big(X_k^*(u;\omega); u \leq s\big)\, ds. \tag{A.1}$$

In conjunction with the process $X_k^*(t;\omega)$, we then define the following empirical CDFs,

$$\widetilde{F}_k^*(\rho_k, x_k;\omega) \triangleq \lim_{T\to\infty} \frac{1}{T}\int_0^T \mathbf{1}\big(p_k(X_k^*(u;\omega); u \leq s) \leq \rho_k\big)\mathbf{1}(X_k^*(s;\omega) \leq x_k)\, ds, \tag{A.2}$$

$$\widetilde{\pi}_k^*(x_k;\omega) \triangleq \lim_{T\to\infty} \frac{1}{T}\int_0^T \mathbf{1}(X_k^*(s;\omega) \leq x_k)\, ds \tag{A.3}$$

$$= \lim_{\rho_k\to\infty} \widetilde{F}_k^*(\rho_k, x_k;\omega). \tag{A.4}$$

Now since $X_k^*(t)$ is ergodic, $\widetilde{F}_k^*(\rho_k, x_k;\omega)$ and $\widetilde{\pi}_k^*(x_k;\omega)$ are well defined, and constant $\mathbb{P}-$almost surely on Ω, *i.e.*,

$$\widetilde{F}_k^*(\rho_k, x_k;\omega) \overset{\mathbb{P}-\text{a.s.}}{=} F_k^*(\rho_k, x_k), \tag{A.5}$$

$$\widetilde{\pi}_k^*(x_k;\omega) \overset{\mathbb{P}-\text{a.s.}}{=} \pi_k^*(x_k), \tag{A.6}$$

[1]For clarity, we make the dependence on $\omega \in \Omega$ explicit.

For the functions $F_k^*(\rho_k, x_k)$, $\pi_k^*(x_k)$ in (A.5) and (A.6) we define the conditional CDF $F_k^*(\rho_k|x_k)$ by

$$F_k^*(\rho_k, x_k) = \int_0^{x_k} F_k^*(\rho_k|s)\pi_k^*(ds). \tag{A.7}$$

Also, we define the memoryless power policy $p_k(x_k)$ as follows

$$p_k(x_k) \triangleq \int_0^{\infty} \rho_k F_k^*(d\rho_k|x_k), \tag{A.8}$$

and a corresponding storage process $X_k(t)$ governed by

$$X_k(t) = X_k(0) + \mathscr{E}_k^{\mathrm{In}}(0,t] - \int_0^t p_k\big(X_k(s)\big)\, ds. \tag{A.9}$$

Also, we denote the stationary measure of $X_k(t)$ by $\pi_k(x_k)$. Our objective now is to prove that the throughput using the storage process with memory $p_k^*(X_k^*(u;w), u \le t)$ is no better than that of it's memoryless counterpart $p_k(X_k(t))$, *i.e.*,

$$\mathcal{R}(\{p_k^*(X_k^*(s;w); s \le t)\}_{k=1}^M) \overset{\mathbb{P}-\text{a.s.}}{\le} \mathcal{R}\big(\{p_k(X_k(t))\}_{k=1}^M\big). \tag{A.10}$$

To show this result, we begin with the definition of the long term average throughput for the storage process in (A.1), *i.e.*,

$$\begin{aligned}
\mathcal{R}\big(\{p_k^*(X_k^*(s;w); s \le t)\}_{k=1}^M\big) &\triangleq \lim_{T\to\infty} \frac{1}{T} \int_0^T r\Big(\sum_{k=1}^M p_k^*(X_k^*(s;w); s \le t)\Big)\, ds &\text{(A.11)}\\
&\overset{(a)}{=} \int_{\mathcal{A}} \int_{\mathcal{B}} r(\sum_{k=1}^M \rho_k) \prod_{k=1}^M \widetilde{F}_k^*(d\rho_k, dx_k; w) &\text{(A.12)}\\
&\overset{\mathbb{P}-\text{a.s.}}{=} \int_{\mathcal{A}} \int_{\mathcal{B}} r(\sum_{k=1}^M \rho_k) \prod_{k=1}^M F_k^*(d\rho_k, dx_k) &\text{(A.13)}\\
&= \int_{\mathcal{A}} \int_{\mathcal{B}} r(\sum_{k=1}^M \rho_k) \prod_{k=1}^M F_k^*(d\rho_k|x_k)\pi_k^*(dx_k), &\text{(A.14)}
\end{aligned}$$

where (a) follows from the definition of $\widetilde{F}_k^*(d\rho_k, dx_k; w)$ in (A.2), and $\mathcal{B} \triangleq [0,\infty) \times [0,\infty) \times \cdots [0,\infty)$ is the domain of integration on $\{\rho_k\}_{k=1}^M$. From concavity of the rate function, we then upper bound (A.14) as follows

$$\mathcal{R}\big(\{p_k^*(X_k^*(s;w); s \le t)\}_{k=1}^M\big) \overset{\mathbb{P}-\text{a.s.}}{=} \int_{\mathcal{A}}\int_{\mathcal{B}} r(\sum_{k=1}^M \rho_k)\prod_{\ell=1}^M F_\ell^*(d\rho_\ell|x_\ell)\prod_{k=1}^M \pi_k^*(dx_k) \tag{A.15}$$

$$\le \int_{\mathcal{A}} r(\sum_{k=1}^M \int_B \rho_k \prod_{\ell=1}^M F_\ell^*(d\rho_\ell|x_\ell))\prod_{k=1}^M \pi_k^*(dx_k) \tag{A.16}$$

$$= \int_{\mathcal{A}} r\big(\sum_{k=1}^M \int_0^\infty \rho_k F_k^*(d\rho_k|x_k)\big)\prod_{k=1}^M \pi_k^*(dx_k) \tag{A.17}$$

$$\triangleq \int_{\mathcal{A}} r\big(\sum_{k=1}^M p_k(x_k)\big)\prod_{k=1}^M \pi_k^*(dx_k), \tag{A.18}$$

where the last step follows from the definition of $p_k\big(x_k\big)$ in (A.8). The remaining task is now to show that $\pi_k^*(x_k) = \pi_k(x_k), \forall k \in [M]$. For this purpose, we define some notation in conjunction with an arbitrary, stationary, *càdlàg*[2] process $Y(t)$ whose jumps (positive or negative) occur at time instants $T^0, T^1, \cdots$. In particular, the right hand derivative of $Y(t)$ is defined by

$$Y^+(t) \triangleq \lim_{\epsilon\downarrow 0}\frac{Y(t+\epsilon)-Y(t)}{\epsilon}. \tag{A.19}$$

In addition, define

$$Y(t^-) \triangleq \lim_{\epsilon\downarrow 0} Y(t-\epsilon). \tag{A.20}$$

Theorem 4 *Let $Y(t)$ be an ergodic, stationary, càdlàg process. Then,*

$$f(y)\mathbb{E}\big[Y^+(t)|Y(t)=y\big] = \lambda^0\mathbb{E}^0\big[\mathbf{1}_{\{Y(T^{0,-})>y\}}\mathbf{1}_{\{Y(T^0)<y\}} - \mathbf{1}_{\{Y(T^{0,-})<y\}}\mathbf{1}_{\{Y(T^0)>y\}}\big], \tag{A.21}$$

where $f(y)$ is the probability density at y, and $\mathbb{E}^0$ denotes the expectation with respect to the Palm probability distribution corresponding to the point process (with assumed intensity λ^0) for the jumps. □

Proof 5 *A proof based on the rate conservation law (RCL) can be found in [28, pp. 36].*

[2]Right continuous with left hand limit. Note that both the storage processes in (A.1) and (A.9) are càdlàg.

Remark 8 *The term* $\mathbf{1}_{\{Y(T^{0,-})>y\}}\mathbf{1}_{\{Y(T^0)<y\}}$ *in the right hand side of Theorem 4 corresponds to negative jumps in the sample path while* $\mathbf{1}_{\{Y(T^{0,-})<y\}}\mathbf{1}_{\{Y(T^0)>y\}}$ *corresponds to positive jumps.*

Remark 9 *As the memoryless storage process in (A.9) only contains positive jumps,*

$$\mathbb{E}^0\left[\mathbf{1}_{\{X_k(T_k^{0,-})>x_k\}}\mathbf{1}_{\{X_k(T_k^0)<x_k\}}\right]=0,$$

where as defined in Section 2.1-B, $T_k^0, T_k^1, \cdots$ *denote the energy arrival times for the* k^{th} *node. In this special case, we then have*

$$\begin{aligned} f_k(x_k)\mathbb{E}[X_k^+(t)|X_k(t)=x_k] &= f_k(x_k)\mathbb{E}[-p_k(X_k(t))|X_k(t)=x_k] && \text{(A.22)}\\ &= -f_k(x_k)p_k(x_k). && \text{(A.23)}\end{aligned}$$

For the right hand side of Theorem 4 we obtain

$$\begin{aligned} \lambda^0\mathbb{E}^0[-\mathbf{1}_{\{X_k(T^{0,-})<x_k\}}\mathbf{1}_{\{X_k(T^0)>x_k\}}] &\overset{(a)}{=} \lambda_k\mathbb{E}[-\mathbf{1}_{\{X_k(T^{0,-})<x_k\}}\mathbf{1}_{\{X_k(T^0)>x_k\}}] && \text{(A.24)}\\ &= -\lambda_k\int_0^{x_k}\big(1-B_k(x_k-v_k)\big)\pi_k(dv_k) && \text{(A.25)}\\ &= -\lambda_k\Big[\big(1-B_k(x_k)\big)\pi_k^0+\int_{0^+}^{x_k}\big(1-B_k(x_k-v_k)\big)f(v_k)\ dv_k\Big], && \text{(A.26)}\end{aligned}$$

where (a) follows from the notion of Poisson Arrivals See Time Averages (PASTA) [28, Prop. 1.23] for Poisson energy arrival process with intensity $\lambda^0=\lambda_k$*. Equating (A.23) and (A.26) according to Theorem 4, we obtain*

$$f_k(x_k)p_k(x_k)=\lambda_k\left[\big(1-B_k(x_k)\big)\pi_k^0+\int_{0^+}^{x_k}\big(1-B_k(x_k-v_k)\big)f_k(v_k)\ dv_k\right], \tag{A.27}$$

which is the equilibrium condition in (2.10) with the density $f_k(x_k)$ *and the atom* π_k^0*.*

Returning to the storage process with memory in (A.1), now it is also easy to see that

$$\begin{aligned} \mathbb{E}\big[(X_k^*(t))^+|X_k^*(t)=x_k\big] &= \int_0^\infty \rho_k F_k(d\rho_k|x_k) && \text{(A.28)}\\ &\triangleq p_k(x_k), && \text{(A.29)}\end{aligned}$$

which is simply the average rate of down crossing at level x_k corresponding to the stationary distribution of $X_k^*(t)$ in (A.1). Applying the same technique as Remark 9 to the process in (A.1), we thus obtain

$$f_k^*(x_k)\mathbb{E}\big[(X_k^*(t))^+ | X_k^*(t) = x_k\big] = f_k^*(x_k)p_k(x_k) \tag{A.30}$$

$$= \lambda_k \left[\big(1 - B_k(x_k)\big)\pi_k^{*,0} + \int_{0^+}^{x_k} \big(1 - B_k(x_k - v_k)\big) f_k^*(v_k)\, dv_k\right], \tag{A.31}$$

where $\pi_k^{*,0}$ and $f_k^*(x_k)$ are the atom and the continuous part (density) of the probability measure $\pi_k^*(x_k)$. Since from Theorem 1 the probability measure that solves (A.27) and (A.31) is unique,

$$\pi_k^*(x_k) = \pi_k(x_k), \quad \forall x_k. \tag{A.32}$$

Concluding from (A.18), we thus showed that

$$\begin{aligned}\mathcal{R}\big(\{p_k^*(X_k^*(s;w); s \le t)\}_{k=1}^M\big) &\overset{\mathbb{P}-\text{a.s.}}{\le} \int_{\mathcal{A}} r\big(\sum_{k=1}^M p_k(x_k)\big)\pi_k^*(dx_k)\\ &= \int_{\mathcal{A}} r\big(\sum_{k=1}^M p_k(x_k)\big)\pi_k(dx_k)\\ &\overset{\mathbb{P}-\text{a.s.}}{=} \mathcal{R}\big(\{p_k(X_k(t))\}_{k=1}^M\big)\end{aligned}$$

Remark 10 *We note that in the ergodic regime, the upcrossing rate as well as the drift component of the storage process in the finite battery case also obey the law stated in Theorem 2. Thus, we again obtain (A.31) as battery overflow does not change the upward and downward rates. Therefore, a similar proof can be used to show $X_k(t)$ is a sufficient statistic for optimal power policies in the storage model with a finite battery capacity (2.7).*

Appendix B

Concavity of the Objective Function Over Each Coordinate

Since for all $k \neq j$,

$$(\pi_k^{0,\alpha}, g_k^\alpha(x_k)) = (\pi_k^{0,1}, g_k^1(x_k)) = (\pi_k^{0,2}, g_k^2(x_k)),$$

we have that

$$\pi_k^\alpha(dx_k) = \pi_k^1(dx_k) = \pi_k^2(dx_k).$$

Then,

$$\mathcal{R}_j^\alpha = \int_{\mathcal{A}} r\left(\lambda_j \frac{G_j^\alpha(x_j)}{g_j^\alpha(x_j)} + \sum_{k \in [M]-j} \lambda_k \frac{G_k(x_k)}{g_k(x_k)}\right) \pi_j^\alpha(dx_j) \prod_{k \in [M]-j} \pi_k(dx_k) \tag{B.1}$$

$$= \mathbb{E}_j\left[\int_0^{L_j} r\left(\lambda_j \frac{G_j^\alpha(x_j)}{g_j^\alpha(x_j)} + \sum_{k \in [M]-j} \lambda_k \frac{G_k(x_k)}{g_k(x_k)}\right) \pi_j^\alpha(dx_j)\right] \tag{B.2}$$

$$= \mathbb{E}_j\left[\int_0^{L_j} r\left(\lambda_j \frac{G_j^\alpha(x_j)}{g_j^\alpha(x_j)} + \sum_{k \in [M]-j} \lambda_k \frac{G_k(x_k)}{g_k(x_k)}\right) [\pi_j^{0,\alpha}\delta(x_j) + e^{-\zeta_j x_j} g_j^\alpha(x_j)] dx_j\right] \tag{B.3}$$

$$= \mathbb{E}_j\left[\int_0^{L_j} r\left(\lambda_j \frac{G_j^\alpha(x_j)}{g_j^\alpha(x_j)} + \sum_{k \in [M]-j} \lambda_k \frac{G_k(x_k)}{g_k(x_k)}\right) e^{-\zeta_j x_j} g_j^\alpha(x_j) dx_j\right] + \pi_j^{0,\alpha} \mathbb{E}_j\left[r\left(\sum_{k \in [M]-j} \lambda_k \frac{G_k(x_k)}{g_k(x_k)}\right)\right]. \tag{B.4}$$

For the term inside the first expectation in (B.4), we proceed as below

$$
\begin{aligned}
&\int_0^{L_j} r\bigg(\lambda_j \frac{G_j^\alpha(x_j)}{g_j^\alpha(x_j)} + \sum_{k\in[M]-j} \lambda_k \frac{G_k(x_k)}{g_k(x_k)}\bigg) e^{-\zeta_j x_j} g_j^\alpha(x_j) dx_j \\
&= \int_0^{L_j} r\bigg(\lambda_j \frac{\alpha G_j^1(x_j) + \bar{\alpha} G_j^2(x_j)}{\alpha g_j^1(x_j) + \bar{\alpha} g_j^2(x_j)} + \sum_{k\in[M]-j} \frac{\lambda_k G_k(x_k)}{g_k(x_k)}\bigg) \left(\alpha e^{-\zeta_j x_j} g_j^1(x_j) + \bar{\alpha} e^{-\zeta_j x_j} g_j^2(x_j)\right)\, dx_j \\
&= \int_0^{L_j} r\bigg(\lambda_j \frac{\alpha e^{-\zeta_j x_j} G_j^1(x_j) + \bar{\alpha} e^{-\zeta_j x_j} G_j^2(x_j)}{\alpha e^{-\zeta_j x_j} g_j^1(x_j) + \bar{\alpha} e^{-\zeta_j x_j} g_j^2(x_j)} + \sum_{k\in[M]-j} \frac{\lambda_k G_k(x_k)}{g_k(x_k)}\bigg) \\
&\times \left(\alpha e^{-\zeta_j x_j} g_j^1(x_j) + \bar{\alpha} e^{-\zeta_j x_j} g_j^2(x_j)\right)\, dx_j \\
&\overset{(a)}{\geq} \int_0^{L_j} r\bigg(\lambda_j \frac{\alpha e^{-\zeta_j x_j} G_j^1(x_j)}{\alpha e^{-\zeta_j x_j} g_j^1(x_j)} + \sum_{k\in[M]-j} \frac{\lambda_k G_k(x_k)}{g_k(x_k)}\bigg) \alpha e^{-\zeta_j x_j} g_j^1(x_j)\, dx_j \\
&+ \int_0^{L_j} r\bigg(\lambda_j \frac{\bar{\alpha} e^{-\zeta_j x_j} G_j^2(x_j)}{\bar{\alpha} e^{-\zeta_j x_j} g_j^2(x_j)} + \sum_{k\in[M]-j} \frac{\lambda_k G_k(x_k)}{g_k(x_k)}\bigg) \bar{\alpha} e^{-\zeta_j x_j} g_j^2(x_j) dx_j \\
&= \alpha \int_0^{L_j} r\bigg(\lambda_j \frac{G_j^1(x_j)}{g_j^1(x_j)} + \sum_{k\in[M]-j} \frac{\lambda_k G_k(x_k)}{g_k(x_k)}\bigg) e^{-\zeta_j x_j} g_j^1(x_j)\, dx_j \\
&+ \bar{\alpha} \int_0^{L_j} r\bigg(\lambda_j \frac{G_j^2(x_j)}{g_j^2(x_j)} + \sum_{k\in[M]-j} \frac{\lambda_k G_k(x_k)}{g_k(x_k)}\bigg) e^{-\zeta_j x_j} g_j^2(x_j) dx_j,
\end{aligned}
$$

where (a) can be verified via lemma given in Appendix C and choosing

$$
\begin{aligned}
a_1 &= \alpha e^{-\zeta_j x_j} g_j^1(x_j), \quad a_2 = \bar{\alpha} e^{-\zeta_j x_j} g_j^2(x_j), \\
b_1 &= \alpha e^{-\zeta_j x_j} G_j^1(x_j), \quad b_2 = \bar{\alpha} e^{-\zeta_j x_j} G_j^2(x_j),
\end{aligned}
$$

and

$$
\gamma = \lambda_j, \qquad \beta = \sum_{k\in[M]-j} \frac{\lambda_k G_k(x_k)}{g_k(x_k)}.
$$

Therefore, for the first term of (B.4) we obtain

$$\begin{aligned}
&\mathbb{E}_j\left[\int_0^{L_j} r\left(\lambda_j \frac{G_j^\alpha(x_j)}{g_j^\alpha(x_j)} + \sum_{k\in[M]-j} \lambda_k \frac{G_k(x_k)}{g_k(x_k)}\right) e^{-\zeta_j x_j} g_j^\alpha(x_j) dx_j\right] \\
&\geq \alpha \mathbb{E}_j\left[\int_0^{L_j} r\left(\lambda_j \frac{G_j^1(x_j)}{g_j^1(x_j)} + \sum_{k\in[M]-j} \lambda_k \frac{G_k(x_k)}{g_k(x_k)}\right) e^{-\zeta_j x_j} g_j^1(x_j) dx_j\right] \\
&+ \bar{\alpha} \mathbb{E}_j\left[\int_0^{L_j} r\left(\lambda_j \frac{G_j^2(x_j)}{g_j^2(x_j)} + \sum_{k\in[M]-j} \lambda_k \frac{G_k(x_k)}{g_k(x_k)}\right) e^{-\zeta_j x_j} g_j^2(x_j) dx_j\right]. \qquad \text{(B.5)}
\end{aligned}$$

Splitting the second term of (B.4) as

$$\begin{aligned}
&\pi_j^{0,\alpha} \mathbb{E}_j\left[r\left(\sum_{k\in[M]-j} \lambda_k \frac{G_k(x_k)}{g_k(x_k)}\right)\right] = \\
&\alpha \pi_j^{0,1} \mathbb{E}_j\left[r\left(\sum_{k\in[M]-j} \lambda_k \frac{G_k(x_k)}{g_k(x_k)}\right)\right] + \bar{\alpha} \pi_j^{0,2} \mathbb{E}_j\left[r\left(\sum_{k\in[M]-j} \lambda_k \frac{G_k(x_k)}{g_k(x_k)}\right)\right], \qquad \text{(B.6)}
\end{aligned}$$

and combining (B.5) and (B.6) we derive

$$\mathcal{R}_j^\alpha \geq \alpha \mathcal{R}_j^1 + \bar{\alpha} \mathcal{R}_j^2. \qquad \text{(B.7)}$$

■

Appendix C

A Lemma

Lemma 2 *Let $\gamma, \beta > 0$, $a_k > 0$ and $b_k > 0$ be given. Then*

$$\sum_k a_k r(\gamma \frac{b_k}{a_k} + \beta) \leq a r(\gamma \frac{b}{a} + \beta), \tag{C.1}$$

where $a = \sum_k a_k$ and $b = \sum_k b_k$. □

Proof 6 *we define the function $V(x) = x r\big((\gamma/x) + \beta\big)$ which is known to be concave for all $x > 0$ since*

$$V''(x) = \frac{\gamma^2}{x^3} r''(\frac{\gamma}{x} + \beta) < 0,$$

where the concavity property of the rate function has been used. We then proceed as

$$\begin{aligned}\sum_k a_k r(\gamma \frac{b_k}{a_k} + \beta) &= \sum_k b_k (a_k/b_k) r(\gamma \frac{b_k}{a_k} + \beta) \\ &= \sum_k b_k V(a_k/b_k) \\ &= b \sum_k (b_k/b) V(a_k/b_k).\end{aligned}$$

Furthermore, from concavity of $V(x)$,

$$\begin{aligned} b\sum_k (b_k/b)V(a_k/b_k) &\leq bV(\sum_k b_k/b \times a_k/b_k) \\ &= bV(a/b) \\ &= ar(\gamma\frac{b}{a} + \beta). \end{aligned}$$

Hence,

$$\sum_k a_k r(\gamma\frac{b_k}{a_k} + \beta) \leq ar(\gamma\frac{b}{a} + \beta).$$

Appendix D

Formulation of Power Policies on a Finite-Time Horizon

Here, we consider the dynamic programming approach to characterize an optimal transmission power policy in a single user communication system ($k = 1$) over the time slot of $[0, T]$ and with the finite battery capacity L. The energy arrival model is assumed to be the same as Section 2.1. However, the storage model (2.7) now takes the following form

$$X(t) = X(0) + \mathscr{E}_k^{\mathrm{In}}(0, t] - \int_0^t p(s, X(s))\, ds, \tag{D.1}$$

where $p(s, X(s))$ is the transmission power that is a function of time and the energy of the battery. We note that t is running up to the exit time from the boundary $x = L$, i.e.,

$$0 \leq t \leq \min\big\{\tau^+(L), T\big\}, \tag{D.2}$$

where $\tau^+(x) := \inf\{t \geq 0 : X(t) \geq x\}$.

***Definition* 3** *The set of admissible power controls, $\pi[t, x]$ at time t and for energy storage value of $X(t) = x$ is defined as the set of 5-tuples $\big(\Omega, \mathcal{F}, \mathbb{P}, \{\mathscr{E}_k^{\mathrm{In}}(0, s]\}_{t \leq s \leq T}, p(\cdot)\big)$ satisfying the following conditions* [1]

- $\big(\Omega, \mathcal{F}, \mathbb{P}\big)$ *is a complete probability space.*

[1] Here, we are only interested in Markov transmission power policies.

- $\{\mathscr{E}_k^{\text{In}}(0,s]\}_{s\geq t}$ *is the arrival process defined on* $(\Omega, \mathcal{F}, \mathbb{P})$ *with filtration* $\mathcal{F}_{[t,s]} = \sigma\{\mathscr{E}^{In}(0,r] : t \leq r \leq s\}$.

- $p(\cdot) : [t,T] \times [0,L] \times \Omega \to \mathbb{R}^+$ *is an* $\{\mathcal{F}_{[t,s]}\}_{t\leq s\leq T}$*-adapted process on* $(\Omega, \mathcal{F}, \mathbb{P})$.

The objective is to maximize the total expected transmission rate over the interval $[0,T]$, i.e.,

$$\sup_{p(\cdot)} \mathbb{E}\left[\int_0^{\min\{\tau^+(L),T\}} r\big(p(s,X(s))\big)\ ds + \psi(X(T))\mathbf{1}_{\{\tau(L)\geq T\}}\right], \tag{D.3}$$

where $\psi(\cdot) : [0,L] \to \mathbb{R}^-$ is the terminal cost function that establishes the penalty of having the residual energy in the battery at the time deadline $t = T$. Now, we define the value functional $V(t,x)$ as follows

$$V(t,x) \triangleq \sup_{p\in\pi[t,x]} \mathbb{E}\left[\int_t^{\min\{\tau^+(L),T\}} r\big(p(s,X(s))\big)\ ds + \psi(X(T))\mathbf{1}_{\{\tau(L)\geq T\}}\right]. \tag{D.4}$$

***Definition* 4** *A two-parameter family of linear operators* $\{T(r,t)\}_{0\leq r,t}$ *is a semigroup if it satisfies*

- $T(r,s)T(s,t) = T(r,t)$ *for all* $r,s,t \geq 0$.

- $T(t,t) = I$ *for all* $t \geq 0$ *where* I *is the unit operator.*

***Definition* 5** *The infinitesimal generator of a family of operators* $[T(u,t)f](x)$ *is defined as*

$$(A_t f)(x) \triangleq \lim_{h\downarrow 0} \frac{1}{h}\left[[T(t,t+h)f(t+h,\cdot)](x) - f(t,x)\right], \tag{D.5}$$

on those functions $f(\cdot)$ *for which the limit exists.*

HJB Equation

From Bellman's principle of dynamic programming we have that

$$V(t,x) = \sup_{p(\cdot)\in\pi[t,x]} \mathbb{E}\left[\int_t^{\min\{\tau^+(L),t+h\}} r\big(p(s,X(s)\big)\ ds + V(t+h, x(t+h))\right], \tag{D.6}$$

which can be transformed into the semigroup form for all $0 \le t \le t+h \le T$ as follows

$$V(t,x) = [T(t,t+h)V(t+h,\cdot)](x), \tag{D.7}$$

where the non-linear semigroup $T(t,t+h)$ is defined as

$$[T(t,t+h)V(t+h,\cdot)](x) := \sup_{p(\cdot)\in\pi[t,x]} \mathbb{E}\left[\int_t^{\min\{\tau^+(L),t+h\}} r\big(p(s,X(s)\big)\ ds + V(t+h, x(t+h))\right] \tag{D.8}$$

From (D.7) and by taking $h \downarrow 0$ we obtain

$$\begin{aligned}\lim_{h\to 0}\frac{1}{h}\Big(V(t,x) - [T_{t,t+h}V(t+h,\cdot)](x)\Big) &\overset{\text{Def.5}}{=} [A_t V(t,\cdot)](x)\\ &= 0.\end{aligned} \tag{D.9}$$

Proposition 2 *The generator of the semigroup $T(u,t)$ in conjunction with the energy storage process $X(t)$ in (D.1) has the Courrège form, i.e.,*

$$[A_t f(t,\cdot)](x) = \partial f(t,z)/\partial t + [G_t f(t,\cdot)](x) \tag{D.10}$$

where for $\bar{p} \triangleq \lim_{s\downarrow t} p(s,X(s))$, G_t is defined as

$$\begin{aligned}[G_t f(t,\cdot)](x) = &\sup_{\bar{p}\in[0,\infty)} \big\{r\big(t,\bar{p}\big) + \bar{p}\partial f(t,x).\partial x\big\}\\ &+ \lambda\int_0^\infty f(t,x+x') - f(t,x)]\big(1 - B(dx')\big),\end{aligned} \tag{D.11}$$

where λ is the energy arrival rate and $B(x) = 1 - \exp(-\zeta x)$.

Proof 7 *See [7, Thm. 3.3.3].*

From Proposition 2 we obtain

$$\frac{\partial V(t,x)}{\partial t} + \sup_{\bar{p}\in[0,\infty)} \big\{ r(\bar{p}) + \bar{p}\frac{\partial V(t,x)}{\partial x} \big\}$$
$$+ \lambda \int_0^{\infty} [V(t, x + x') - V(t,x)]\big(1 - B(dx')\big) = 0. \tag{D.12}$$

This is the Hamilton-Jacobi-Bellman equation for optimal power control $p(\cdot)$ with boundary condition $V(x,t)|_{t=T} = \psi(x)$.The optimal power policy is thus the solution to the following problem

$$p^{\text{Optimal}}(\cdot) \in \arg \sup_{\bar{p}\in[0,\infty)} \big\{ r(\bar{p}) + \bar{p}\frac{\partial V(t,x)}{\partial x} \big\}. \tag{D.13}$$

Remark 11 *The PDE in* (D.12) *does not have a classical solution in the sense that there are some points* $(t,x) \in [0,T] \times [0,L]$ *for which* $V(t,x)$ *is not differentiable. Therefore,* $V(t,x)$ *is the general solution (viscosity solution) of* (D.12) *(ref. [16]).*

References

[1] http://en.wikipedia.org/wiki/Sunlight.

[2] http://science.nasa.gov/science-news/science-at-nasa/2002/solarcells.

[3] http://www.ise.fraunhofer.de/.

[4] http://www.nrel.gov/ncpv/.

[5] C. Alippi, G. Anastasi, M. Di Francesco, and M. Roveri. Energy management in wireless sensor networks with energy-hungry sensors. *Instrumentation Measurement Magazine, IEEE*, 12(2):16–23, April 2009.

[6] C. Alippi, G. Anastasi, C. Galperti, F. Mancini, and M. Roveri. Adaptive sampling for energy conservation in wireless sensor networks for snow monitoring applications. In *Proc. IEEE MASS*, Pisa, Italy, October 2007.

[7] David Appelebaum. *Lévy Processes and Stochastic Calculus*. Cambridge University Press, New York, 2004.

[8] S. Asmussen. *Applied probability and queues*. Wiley, New York, 1987.

[9] Patrice Bertail, Stéphan Clémençon, and Jessica Tressou. A storage model with random release rate for modeling exposure to food contaminants. Working Papers 2006-20, Centre de Recherche en Economie et Statistique, 2006.

[10] D. P. Bertsekas. *Nonlinear Programming*. Athena Scientific, Belmont, MA, 1999.

[11] Sid Browne and Karl Sigman. Work-modulated queues with applications to storage processes. *Journal of Applied Probability*, 29(3):699–712, 1992.

[12] A. De Vos and H. Pauwels. On the thermodynamic limit of photovoltaic energy conversion. *Applied Physics*, 25:119–125, 1981.

[13] A. De Vos and H. Pauwels. Efficiency of energy conversion for a piezoelectric power harvesting system. *Journal of Micromechanics and Microengineering*, 16:2429–2438, 2006.

[14] A. Deshpande, C. Guestrin, S. Madden, J. M. Hellerstein, and W. Hong. Model-driven data acquisition in sensor networks. In *Proc. International Conference on Very Large Data Bases (VLDB)*, Toronto-Canada, 2004.

[15] B. Devillers and D. Gündüz. A general framework for the optimization of energy harvesting communication systems with battery imperfections. *Journal of Communications and Networks*, 14(2):130 –139, april 2012.

[16] Wendell H. Fleming and H. Mete Soner. *Controlled Markov Processes and Viscosity Solutions.* Springer, New York, 2 edition, 2006.

[17] D. Ganesan, A. Cerpa, W. Ye, Y. Yu, J. Zhao, and D. Estrin. Networking issues in wireless sensor networks. *Journal of Parallel and Distributed Computing*, 64:799–814, 2004.

[18] DP Gaver and RG Miller. Limiting distributions for some storage problems. *Studies in Applied Probability and Management Science*, pages 110–126, 1962.

[19] JamesM. Gilbert and Farooq Balouchi. Comparison of energy harvesting systems for wireless sensor networks. *International Journal of Automation and Computing*, 5:334–347, 2008.

[20] Fabrice Guillemin and Ravi Mazumdar. Rate conservation laws for multidimensional processes of bounded variation with applications to priority queuing systems. *Methodology and Computing in Applied Probability*, pages 135–159, October 2004.

[21] V.C. Gungor and G.P. Hancke. Industrial wireless sensor networks: Challenges, design principles, and technical approaches. *IEEE Transactions on Industrial Electronics*, 56(10):4258–4265, 2009.

[22] B. Gurakan, O. Ozel, Jing Yang, and S. Ulukus. Energy cooperation in energy harvesting wireless communications. In *Proc. IEEE International Symposium on Information Theory (ISIT), Cambridge, MA*, pages 965–969, july 2012.

[23] T. C. Harman, P. J. Taylor, D. L. Spears, and M. P. Walsh. Thermoelectric quantum-dot superlattices with high ZT. *Journal of Electronic Materials*, 29:L1–L2, 2000.

[24] J.M. Harrison and S.I. Resnick. The stationary distribution and first exit probabilities of a storage process with general release rule. *Mathematics of Operations Research*, 1(4):347–358, 1976.

[25] R. Kroon, M. Lenes, J. C. Hummelen, P. W. M. Blom, and B. de Boer. Small bandgap polymers for organic solar cells (polymer material development in the last 5 years). *Polymer Reviews*, 48(3):531–582, April 2008.

[26] P. Linz. *Analytical and Numerical Methods for Volterra Equations.* Society for Industrial and Applied Mathematics (SIAM), Philadelphia, PA., 1985.

[27] L. Mateu and F. Moll. Review of energy harvesting techniques and applications for microelectronics. In *Proc. Society of Photo-Optical Instrumentation Engineers (SPIE) Microtechnologies for the New Millenium*, 2005.

[28] R. Mazumdar. *Performance Modeling, Loss Networks, and Statistical Multiplexing.* Morgan and Claypool, January 2010.

[29] P. Mitran. On optimal online policies in energy harvesting systems for compound poisson energy arrivals. *in Proc. IEEE International Symposium on Information Theory (ISIT), Cambridge, MA*, pages 960 – 964, 2012.

[30] P.A.P. Moran. A probability theory of dams and storage systems. *Aust. Jour. App. Sci.*, 5:116–124, 1954.

[31] O. Ozel, K. Tutuncuoglu, Jing Yang, S. Ulukus, and A. Yener. Transmission with energy harvesting nodes in fading wireless channels: Optimal policies. *IEEE Journal on Selected Areas in Communications*, 29(8):1732 –1743, 2011.

[32] O. Ozel and S. Ulukus. Information-theoretic analysis of an energy harvesting communication system. In *IEEE 21st International Symposium on Personal, Indoor and Mobile Radio Communications Workshops (PIMRC Workshops)*, pages 330 –335, sept. 2010.

[33] O. Ozel and S. Ulukus. Achieving AWGN capacity under stochastic energy harvesting. *IEEE Transactions on Information Theory*, 58(10):6471 –6483, oct. 2012.

[34] Francisco J. Piera, Ravi R. Mazumdar, and Fabrice M. Guillemin. Boundary behavior and product-form stationary distributions of jump diffusions in the orthant with state-dependent reflections. *Advances in Applied Probability*, 40(2):529–547, 2008.

[35] V. Sharma, U. Mukherji, and V. Joseph. Efficient energy management policies for networks with energy harvesting sensor nodes. In *Allerton Conf. On Communication, Control, and Computing*, pages 375–383, 2008.

[36] E. Shih, P. Bahl, and M. Sinclair. Wake on wireless: An event driven energy saving strategy for battery operated devices. In *Proceedings of the ACM/IEEE International Conference on Mobile Computing and Networking (Mobicom)*, Atlanta, GA, 2002.

[37] A. Singh, D. Budzik, W. Chen, M. A. Batalin, M. Stealey, H. Borgstrom, and W. J. Kaiser. Multiscale sensing: A new paradigm for actuated sensing of high frequency dynamic phenomena. In *Proc. IEEE/RSJ International Conference on Intelligent Robots and Systems (IROS 2006)*, Beijing (China), October 2006.

[38] R. Srivastava and C. E. Koksal. Basic performance limits and tradeoffs in energy-harvesting sensor nodes with finite data and energy storage. *IEEE/ACM Transactions on Networking*, 2012.

[39] M. K. Stojčev, M. R. Kosanović, and L. R. Golubović. Power management and energy harvesting techniques for wireless sensor nodes. In *Proc. 9th IEEE International Conference on Telecommunication in Modern Satellite, Cable, and Broadcasting Services, Nis*, 2009.

[40] Yu-Chee Tseng, Yen-Ning Chang, and Bour-Hour Tzeng. Energy-efficient topology control for wireless ad hoc sensor networks. *Journal of Information Science and Engineering*, 20:27–37, 2004.

[41] K. Tutuncuoglu and A. Yener. Sum-rate optimal power policies for energy harvesting transmitters in an interference channel. *Journal of Communications and Networks*, 14(2):151 –161, april 2012.

[42] Jing Yang, O. Ozel, and S. Ulukus. Broadcasting with an energy harvesting rechargeable transmitter. *IEEE Transactions on Wireless Communications*, 11(2):571 –583, february 2012.

[43] Jing Yang and S. Ulukus. Transmission completion time minimization in an energy harvesting system. In *44th Annual Conference on Information Sciences and Systems (CISS)*, pages 1 –6, march 2010.

[44] Jing Yang and S. Ulukus. Optimal packet scheduling in a multiple access channel with rechargeable nodes. In *Proc. IEEE International Conference on Communications (ICC)*, pages 1–5, june 2011.

[45] Adamu Murtala Zungeru, Li-Minn Ang, SRS. Prabaharan, and Kah Phooi Seng. Radio frequency energy harvesting and management for wireless sensor networks. *arXiv:1208.4439*, 2012.